

[Redacted]

066-4376

(Unclassified Title)

T- 421

SYSTEM TEST DETERMINATION  
OF APOLLO IRIG DRIFT COEFFICIENTS

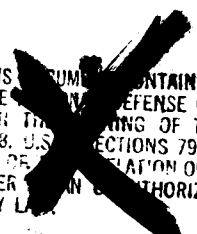
by

George Thomas Schmidt

Submitted in Partial Fulfillment  
of the Requirements for the  
Degree of Master of Science  
at the  
Massachusetts Institute of  
Technology  
June 1965

**CLASSIFICATION CHANGE**  
To UNCLASSIFIED  
By authority of *[Signature]*  
Changed by *[Signature]*  
Classified Document Master Control Station, NASA  
Scientific and Technical Information Facility  
Date *12/11/72*

NOTICE — THIS DOCUMENT CONTAINS INFORMATION AFFECTING THE NATIONAL DEFENSE OF THE UNITED STATES WITHIN THE MEANING OF THE ESPIONAGE LAWS, TITLE 18, U.S. CODE, SECTIONS 793 AND 794. ITS TRANSMISSION OR REVELATION OF ITS CONTENTS IN ANY MANNER TO AN UNAUTHORIZED PERSON IS PROHIBITED BY LAW.



Signature of Author ..... *George T. Schmidt* .....  
Department of Aeronautics & Astronautics  
May 21, 1965

Certified by ..... *Wallace E. Vand Wilde* .....  
Thesis Supervisor

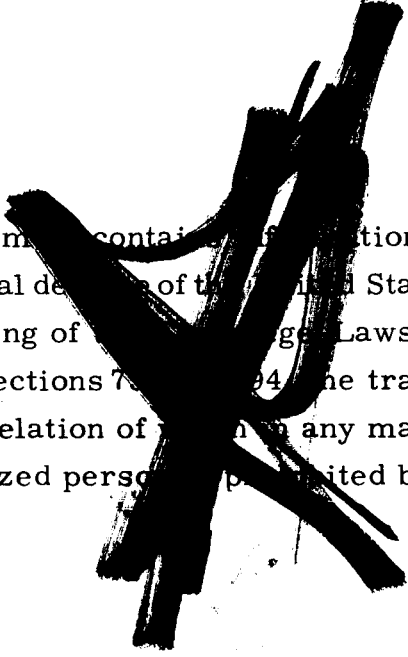
Accepted by ..... *[Signature]* .....  
Chairman, Departmental Committee  
on Graduate Students

[Redacted]

[Redacted]

GROUP 4  
Do not down grade or  
declassify  
after 12 years

This report was prepared under DSR Project 55-238 sponsored by the Manned Spacecraft Center of the National Aeronautics and Space Administration through Contract NAS 9-4065.



This document contains information affecting the national defense of the United States within the meaning of the Espionage Laws, Title 18, U.S.C., Sections 793 and 794, the transmission or the revelation of which in any manner to an unauthorized person is prohibited by law.

The publication of this report does not constitute approval by the Instrumentation Laboratory or the National Aeronautics and Space Administration of the findings or the conclusions contained therein. It is published only for the exchange and stimulation of ideas.

T - 421

SYSTEM TEST DETERMINATION  
OF APOLLO IRIG DRIFT COEFFICIENTS

by

George Thomas Schmidt

Submitted to the Department of Aeronautics and Astronautics  
on May 21, 1965, in partial fulfillment of the requirements for the  
degree of Master of Science.

ABSTRACT

A method of determining the drift coefficients of the gyroscopes in the Apollo Guidance and Navigation System is presented. The technique requires the guidance computer to perform optimum statistical filtering on the east accelerometer output for a freely drifting stable platform. By using computer simulations of the Apollo System coupled with the test procedure, it is shown that the drift of the south gyro can be determined under both laboratory and launch pad environments with a significant improvement over existing test procedures. The drift coefficients of each gyro are found from a series of platform positions.

Thesis Supervisor: Wallace E. Vander Velde

Title: Professor of Aeronautics  
and Astronautics

## ACKNOWLEDGEMENTS

The author wishes to acknowledge the assistance and advice of a number of individuals who made this thesis possible: Professor Wallace E. Vander Velde for supervising the thesis; Mr. Leonard S. Wilk for allowing the thesis work to be done in the Apollo System Test Group of the MIT Instrumentation Laboratory; Mr. Ain Laats for assistance in the laboratory work; Mr. Pieter Mimno for his help in the revisions of G&N system simulation programs and to Miss Frances Sainato for typing drafts and the final copy of the thesis. The author also wishes to acknowledge the substantial advice from his friends and colleagues at the Instrumentation Laboratory.

## TABLE OF CONTENTS

### CHAPTER

	Page
1. Introduction	1
1.1 Statement of the Problem	1
1.2 General Description of the Apollo IMU	2
1.3 Description of the Thesis	8
2. Analytical Derivations	12
2.1 Linearized Platform Dynamics	13
2.2 PIPA Outputs	17
2.3 Error Sources	19
2.4 Least Squares Curve Fitting	22
2.5 Recursive Measurement Theory	25
2.6 The Measurement Vector	30
2.7 Measurement Error	31
2.8 The Optimum Weighing Vector	32
2.9 Extrapolation of $\hat{\mathbf{E}}^*$ and $\hat{\mathbf{x}}$	35
2.10 Platform Positions	43
2.11 Implementation	48
2.12 Chapter Summary	51
3. Computer Simulations	52
3.1 Computer Program Description	53
3.2 Simulation Results	54
3.3 Conclusions from the Simulation Studies	66
4. Conclusions and Summary	67
Appendix A Demonstration Program	69
References	70

## LIST OF ILLUSTRATIONS AND GRAPHS

<u>Figures</u>		Page
1-1	Axes Definition	3
1-2	Stabilization Loops	4
1-3	25 IRIG	5
1-4	IRIG Axes	5
1-5	16 PIP	9
1-6	Stable Member Geometry	10
2-1	Recursive Operations	29
2-2	Pulse Search and Update	41
2-3	Initial Conditions	41
2-4	Integrate $\hat{\mathbf{x}}$	42
2-5	Compute $\hat{\mathbf{N}}, \underline{\mathbf{b}}$	42
2-6	Integrate $\hat{\mathbf{E}}$	42
2-7	Compute Weighing Vector and Step Change in Correlation Matrix	42
2-8	Test Positions	44
 <u>Graphs</u>		
1	Effects of Misalignments	55
2	Effects of PIPA Bias	57
3	Incorrect Measurement Variance	58
4	Incorrect Initial Correlation Matrix	60
5	Missile Motion	61
6	Velocity Estimation	62
7	Launch Pad Estimation	63

## GENERAL NOTATION

Underlining a symbol indicates a column vector.

A bar over a symbol is the average value of the quantity.

An asterisk over a capital letter denotes a matrix.

Superscript T following a vector or matrix indicates the transpose of the vector or matrix.

Superscript -1 following a square matrix indicates the inverse.

$\wedge$  over a quantity indicates an estimate of the quantity.

$\sim$  over a quantity is the measured value of the quantity.

## ERRATA

Throughout this thesis the author uses weighing vector in place of the more common usage of weighting vector.

~~CONFIDENTIAL~~

## CHAPTER 1

### INTRODUCTION

#### 1.1 Statement of the Problem

Numerous methods are available for the calibration of high quality gyroscopes to be used in inertial navigation systems. Testing of the gyroscope at the component level is generally able to achieve an accuracy of at least one meru (one-thousandth of earth rate) in determining the average value of gyro drift during the testing period. However, once the gyro has been installed on an inertial platform in a system, the calibration problem involves an attempt to correlate inertial system performance with the accuracy of a specific component. At present, methods do exist which are able to determine to an accuracy of two meru the gyro drift when the Apollo System is in the laboratory. However, once the system is installed in the Apollo Command Module atop the Saturn launch vehicle, the present test is subject to errors due to wind induced vehicle sway and the accuracy of the test is estimated as  $\pm 50$  meru. (reference 9) An accurate test method is needed that will measure gyro drift in an inertial system in a hostile environment.

This thesis will consider in detail the question of determining the drift of the gyros in the MIT Apollo G&N System while the system

~~CONFIDENTIAL~~



is in the laboratory or installed in the command module atop a Saturn booster prior to launch. It is hoped that the drift test developed will be applicable to a wider variety of inertial systems than the Apollo G&N System.

## 1.2 General Description of the Apollo IMU

This section will briefly describe the mechanization and instrumentation of the Apollo inertial measurement unit (IMU). The description of the gyroscopes and accelerometers in the system will be somewhat detailed since this thesis will propose the measurement of gyro drift by use of the accelerometers.

The IMU is a three-degree-of-freedom stabilized platform consisting of the stable member (SM), three gimbals, gimbal-mounted electronics, and six inter-gimbal assemblies which house torque motors and angular resolvers. The IMU is designed to provide an inertial space reference for the stable member regardless of spacecraft motion. An inertial reference integrating gyroscope (IRIG) and a pulsed integrating pendulous accelerometer (PIPA) are mounted along each of three orthogonal stable member axes. The definitions of gimbal angles and stable member axes are given in Figure 1-1. At zero gimbal angles the three gimbals are orthogonal.

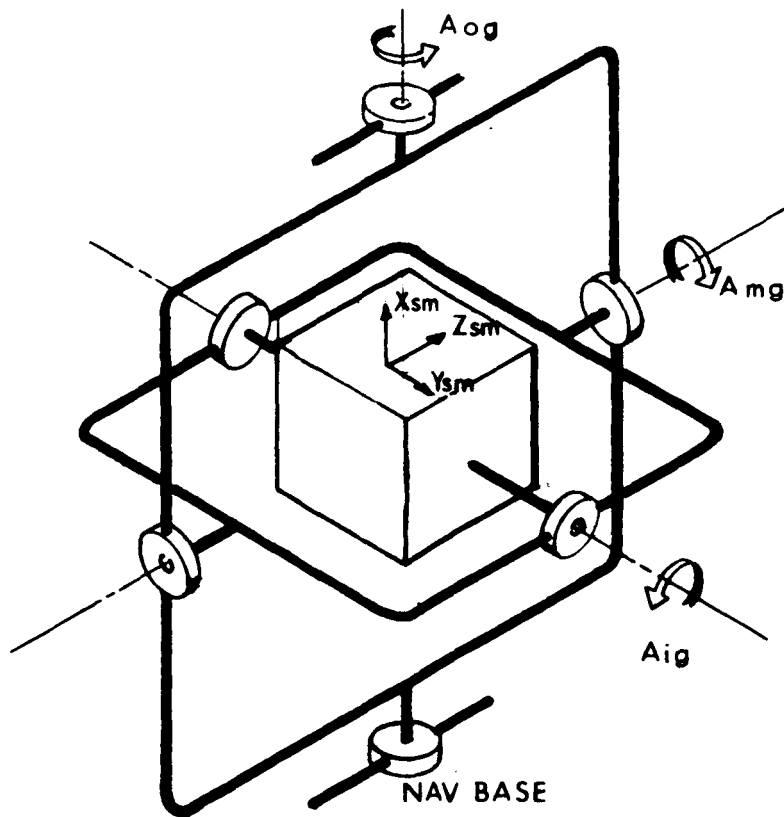


Figure 1-1 Axes Definition

Three stabilization loops maintain the orientation of the three PIPAs fixed with respect to inertial space within limits under all specified external disturbances. If the SM were perfectly instrumented (no gyro drift or other errors), then the SM axes would always maintain the same inertial attitude. The stabilization loops operate as follows: the three IRIGs and three angular differentiating accelerometers (one on the stable member, two on the middle gimbal) generate error signals whenever the SM is rotated with respect to inertial space. The error signals are amplified, resolved if necessary, and supplied to the gimbal torque motors which drive the stable member back to its original position to reduce the error signals to zero. The path of the error signals originating at the IRIGs and terminating at the torque motors is shown in Figure 1-2.

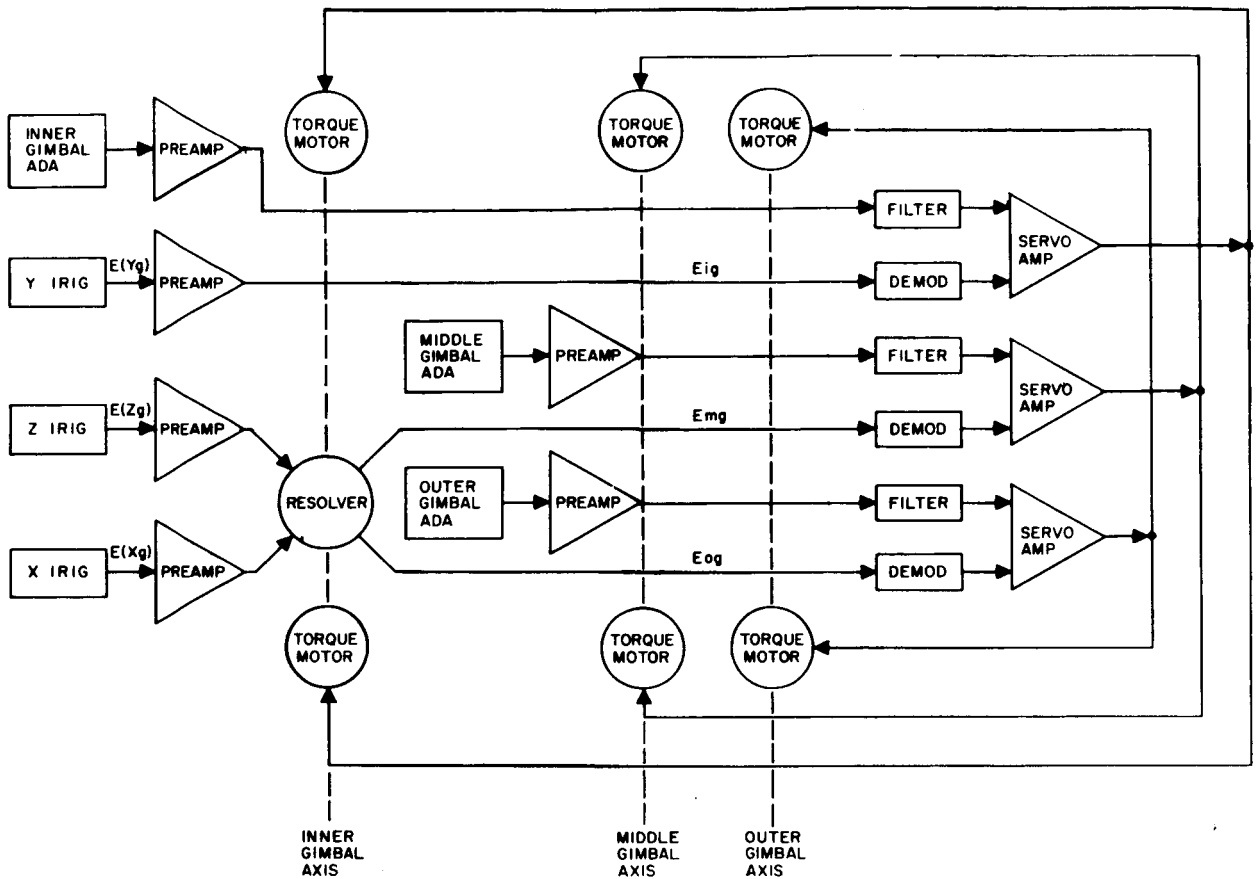


Figure 1-2 Stabilization Loops

The stabilization gyros used in the IMU are 25 IRIGs (25 denoting the case diameter in tenths of inches). This gyro is a fluid and magnetically suspended, single-degree-of-freedom gyro. It uses ducosyns for signal and torque generation. The wheel assembly is driven as an hysteresis **synchronous** motor in an atmosphere of helium to prevent rusting of the ferrous parts. Figures 1-3 and 1-4 illustrate the components within the instrument and define the IRIG axes.

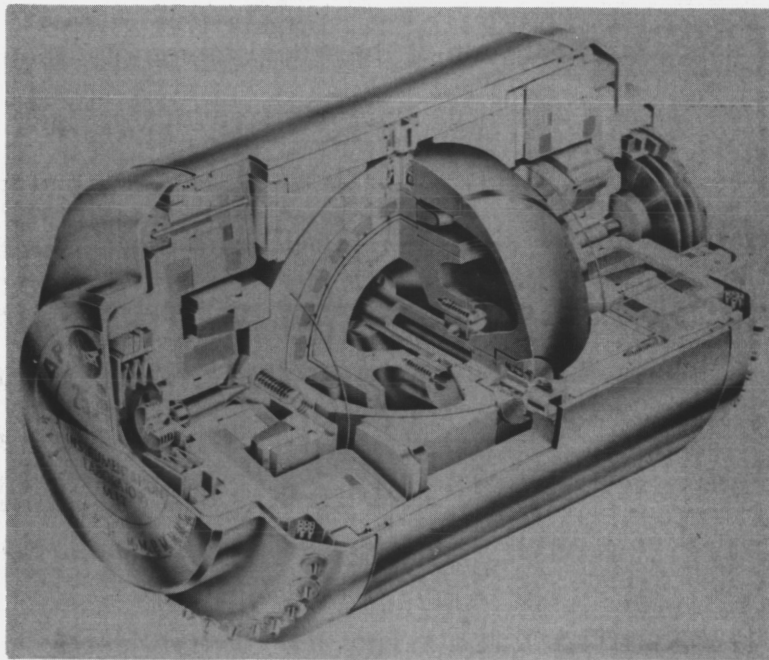


Figure 1-3 25 IRIG

ANGULAR ACCELERATION OF CASE WITH RESPECT TO INERTIAL SPACE ABOUT THE OUTPUT AXIS

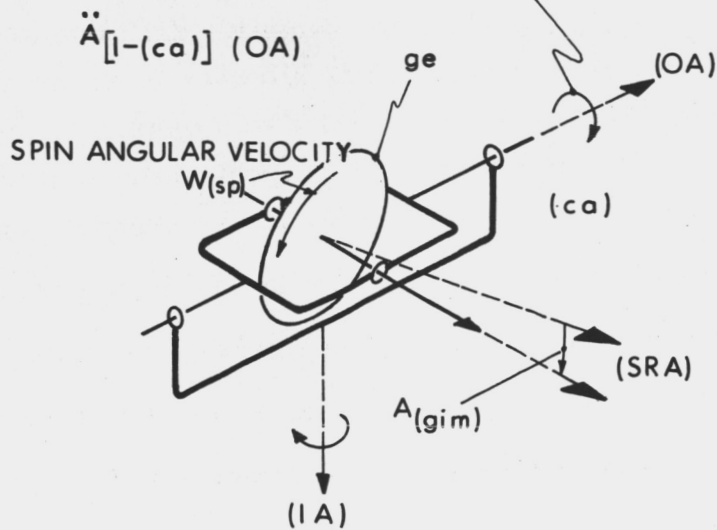


Figure 1-4 IRIG Axis

A positive rotation of the wheel assembly about the gyro output axis develops a signal generator secondary voltage that is in-phase with the primary excitation voltage. A negative rotation produces a 180 degree out of phase signal. This defines the output axis polarity. A positive rotation of the gyro case about the input axis (IA) will produce an in-phase signal generator voltage. The gyro drift coefficients that must be determined are defined as follows:

NBD - The normal excitation bias drift is defined as positive if it causes a negative torque about the output axis. It is non-acceleration sensitive.

ADSRA - The acceleration sensitive drift due to a case acceleration of one gravity along the positive spin reference axis (or gravity along the minus spin reference axis). It is positive if it causes a negative torque about the output axis. Internally, this term is caused by a displacement of the center of gravity with respect to the center of buoyancy of the float along the minus input axis.

ADIA - The acceleration sensitive drift due to a case acceleration of one gravity along the positive gyro input axis. This term is due to a displacement of the center of gravity with respect to the center of buoyancy along the positive spin reference axis.

Drift coefficients which depend on higher powers of the case acceleration are neglected for system test purposes. In general the drift coefficients experience only long term variations; for the purpose of this thesis, the drift coefficients are assumed to be constant during any test (six minutes).

This description of the IRIG and its operation is sufficient for our needs. We will now consider the PIPA.

The 16 PIP is a pulsed pendulum type of accelerometer. An acceleration along the sensitive axis is sensed, integrated, quantized and sent to the Apollo Guidance Computer (AGC) as an increment of velocity. The 16 PIP consists of a pendulous mass unbalance (pendulous float) pivoted with respect to the case. The axis of the case defines the output axis. A 2-volt rms, 3200 cps, single-phase excitation is supplied by the AGC for the PIPA magnetic suspension and primary of the signal generator. With an acceleration being sensed along the input axis, the float rotates from the null position, the rotation is sensed by the signal generator ducosyn and a signal proportional to the rotation is developed. Through various torquing networks the float is torqued back to null. For our purposes the operation of the accelerometer loop may be represented by the following equation:

$$dN/dt = \underline{a} \cdot \underline{i}/H \tag{1.1}$$

where

$dN/dt$  = average PIPA pulse rate output

$\underline{a}$  = acceleration vector

$\underline{i}$  = unit vector in direction of input axis

$\underline{a} \cdot \underline{i}$  = component of acceleration along the input axis

$H$  = nominal scale factor 5.85 cm/sec/pulse

The pulses are counted by the AGC in a special register; at any time a measure of the total velocity increment during a period of time

~~CONFIDENTIAL~~

is available in this register. The effect of quantization on the signal can be eliminated by programming the AGC to store the time that the velocity register changed from one state to the next state and storing the new state. Throughout this thesis this method is used to eliminate a source of error that would be large in the gyro drift tests.

These descriptions of the inertial components and the stabilization loops are sufficient for our purposes. The next two figures show the PIPA and the position of the IRIGs and PIPAs on the stable member. Section 1-3 will then serve as a general introduction to the gyro drift test method proposed in Chapter 2.

### 1.3 Description of the Thesis

The goal of the thesis is a gyro drift coefficient test accuracy of one meru under conditions of both laboratory testing and launch vehicle base motion. The length of time required for the test has been considered of secondary importance. The test should be capable of full automation by the AGC and should be independent of any external reference for the stable member. Since the available computer storage and program files are at a minimum, the test procedure should be accomplished with the minimum of implementation. With these considerations in mind, the proposed solution should be the simplest one that will meet the accuracy requirements.

The author considered a number of different methods for solution of the problem with the use of accelerometer information only. In this procedure, the gyro drift is measured while the stable member is attempting, by means of the stabilization loops, to maintain a fixed

~~CONFIDENTIAL~~

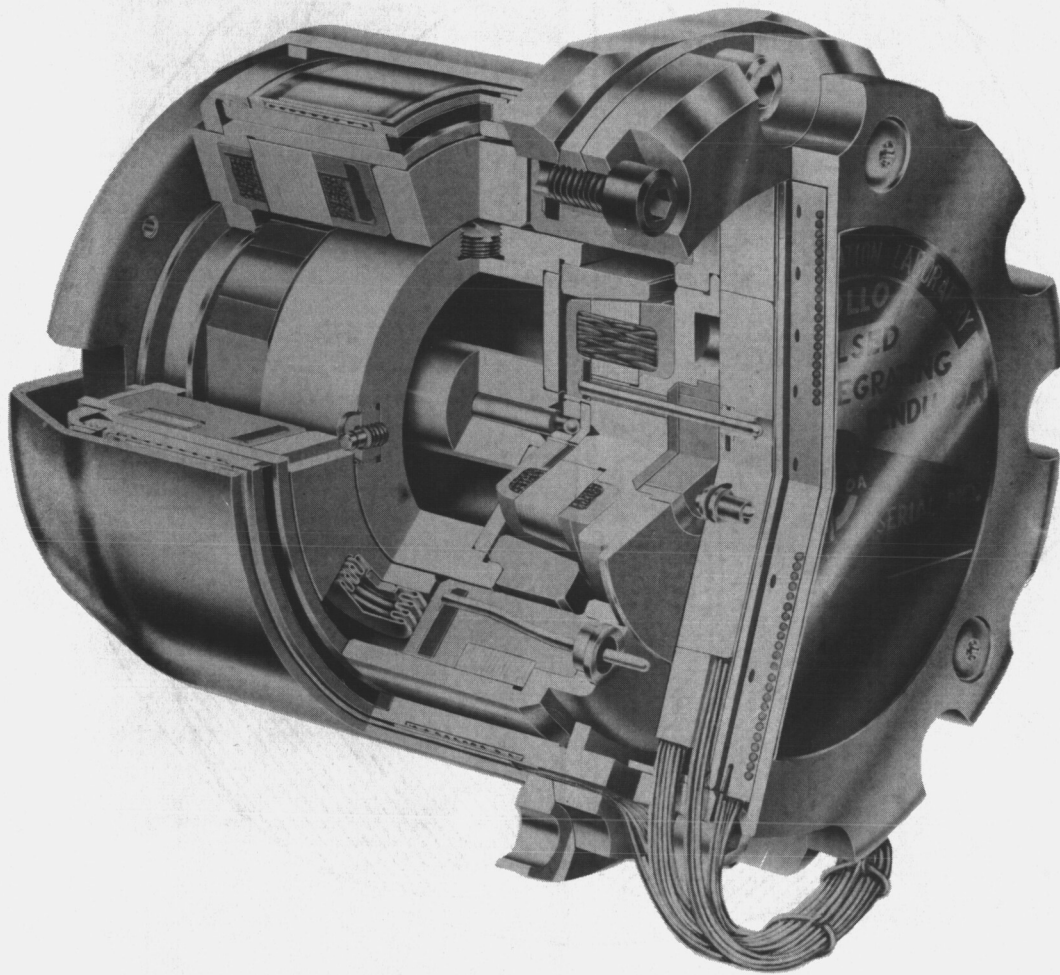


Figure 1-5 16 PIP



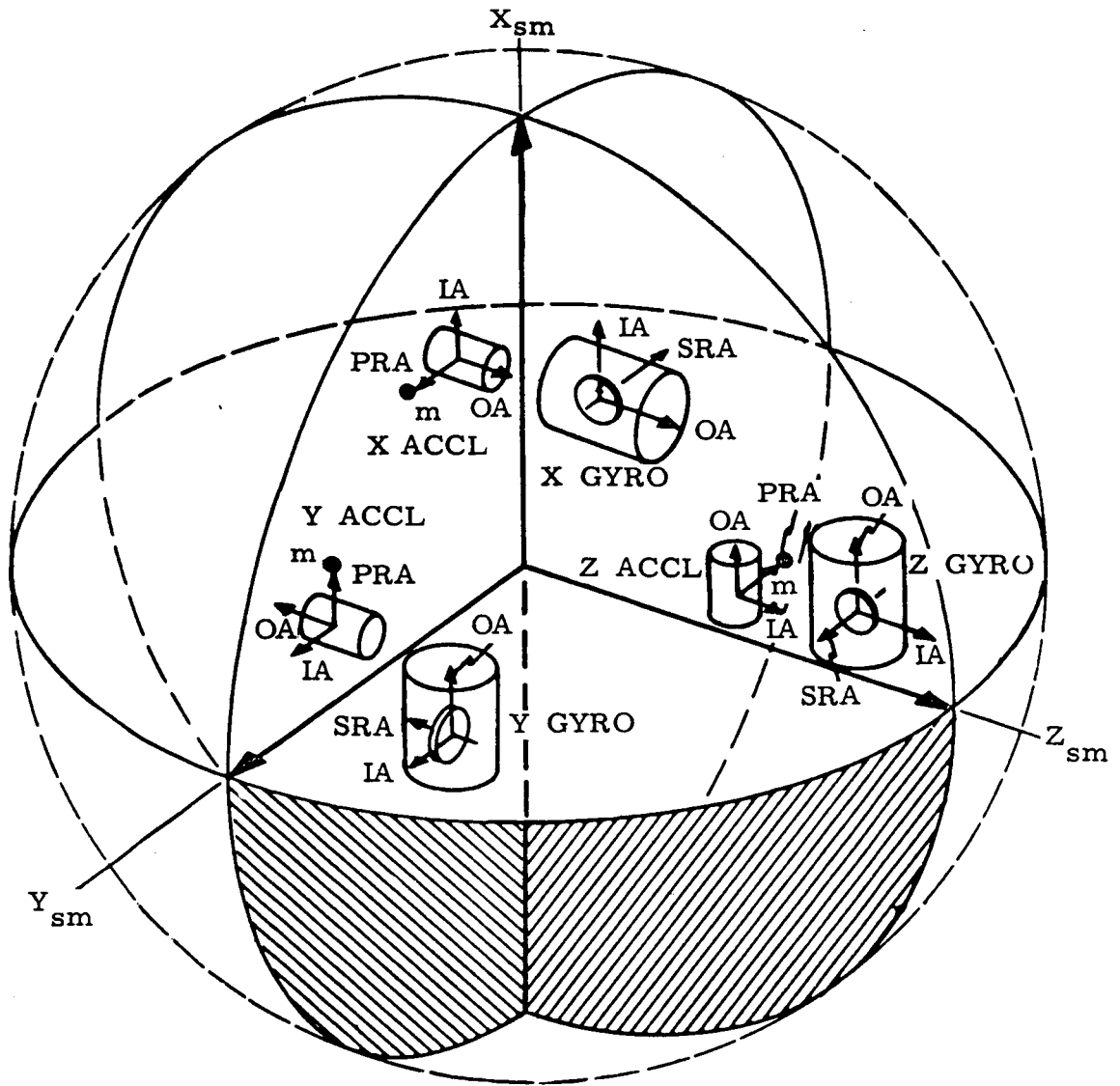


Figure 1-6

Stable Member Geometry

orientation in inertial space. Because of gyro drift the platform drifts from its desired orientation and the PIPA outputs contain information about the drift of the platform in the gravity field. Once the relationships between accelerometer outputs and gyro drifts are determined, it becomes a question of how to use this information in the best (the optimum from a mean squared error criterion) way. For laboratory testing an assumption of normally distributed errors is valid and the least squares estimate of the drift obtained from curve fitting is the maximum likelihood estimate. This assumption is shown not valid for launch pad testing; then the optimum solution to the problem can be formulated as the so-called "Kalman Filter" in which the PIPA data is processed as it is measured to form a new estimate of gyro drift and four other variables which describe the problem.

Chapter 2 of the thesis is concerned with the analytical derivations of the drift test; Chapter 3 describes the computer simulations that were made in the computation center of the Instrumentation Laboratory. The results of these simulations indicate that the test procedure will be an effective method under all expected environments.

## CHAPTER 2

### ANALYTICAL DERIVATIONS

In this chapter the analytical developments leading to the proposed gyro drift coefficient test will be derived. First, the relationships among platform motion, accelerometer output, and gyro drift are derived. Then the existing test methods are rejected for use when the launch vehicle is subject to wind induced sway. After determining that the method of least squares curve fitting will not prove effective, the final test procedure is derived from statistical filtering theory. The test method processes the data (PIPA pulse counts) recursively to form a new estimate of the state vector and the correlation matrix of the errors in the estimate after each piece of data is received. The state vector has as its components the variables and constants that must be estimated if we are to determine gyro drift. The chapter concludes with an estimate of the computer storage that would be required to implement the test.

## 2.1 Linearized Platform Dynamics

In order to relate PIPA outputs to IRIG drifts, we must first determine the motion of the platform in the gravity field as the stable member attempts to maintain a constant inertial attitude.

Consider first that the platform is aligned to some known initial orientation. The only constraint on this initial alignment is that the platform is not near a position of gimbal lock (the Y stable member axis vertical). The platform then goes inertial; at some later time the platform will have rotated from its initial orientation in the gravity field because of gyro drift, earth rate, and errors in the stabilization loops. To be sure, the main contributor to the rotation is earth rate; the problem is to separate the effects of gyro drift from the error sources. The rotations will be small for the short duration of the test; hence, a linear analysis of the platform dynamics seems possible. The transformation matrix that transforms components of a vector in the initial orientation coordinates to the stable member coordinates is given by

$$\underline{V}_{sm} = \begin{bmatrix} 1 & 0 & 0 \\ 0 & \cos Ax & \sin Ax \\ 0 & -\sin Ax & \cos Ax \end{bmatrix} \begin{bmatrix} \cos Az & \sin Az & 0 \\ -\sin Az & \cos Az & 0 \\ 0 & 0 & 1 \end{bmatrix} \begin{bmatrix} \cos Ay & 0 & -\sin Ay \\ 0 & 1 & 0 \\ \sin Ay & 0 & \cos Ay \end{bmatrix} \underline{V}_{ref} \quad (2.1)$$

where the rotations are made about the stable member axes (y, z, x) in that order by angles Ay, Az, and Ax.

For small angles

$$\underline{V}_{sm} = \begin{bmatrix} 1 & A_z & -A_y \\ -A_z & 1 & A_x \\ A_y & -A_x & 1 \end{bmatrix} \underline{V}_{ref} \quad (2.2)$$

or

$$\underline{V}_{sm} = \overset{*}{A} \text{rot} \underline{V}_{ref} \quad (2.3)$$

In an ideal platform each IRIG will have its input axis along a stable member axis. In general, however, a set of misalignment vectors exist which define the actual direction of the IRIG axes with respect to the stable member axes. Then a vector in stable member coordinates would transform into one in the IRIG input axis coordinate system by the IRIG misalignment matrix  $\overset{*}{\gamma}_{mis}$

$$\underline{V}_{irig} = \begin{bmatrix} 1 & \gamma_{xz} & -\gamma_{xy} \\ -\gamma_{yz} & 1 & \gamma_{yx} \\ \gamma_{zy} & -\gamma_{zx} & 1 \end{bmatrix} \underline{V}_{sm} \quad (2.4)$$

or

$$\underline{V}_{irig} = \overset{*}{\gamma}_{mis} \underline{V}_{sm} \quad (2.5)$$

$\gamma_{ij}$  is the rotation of the i IRIG about the j stable member axis. The  $\gamma_{ijs}$  are small (.001 radians).

Each IRIG indicates an angular velocity which is the sum of earth rate along that axis and drift of that gyro.<sup>1</sup> This indicated angular velocity is transformed into rotations of the stable member axes by the stabilization loops and because the platform is inertial the angular velocity of the stable member is

$$\underline{W}_{sm} = -\overset{*}{\gamma}^{-1}_{mis} \underline{W}_{irig} \quad (2.6)$$

<sup>1</sup> - Angular velocity with respect to inertial space.

The angular velocity indicated by the IRIGs is given by

$$\underline{W}_{irig} = \gamma^* \text{mis} \dot{A} \text{rot} \underline{W}_{ref} - \underline{D} \quad (2.7)$$

where  $\underline{W}$  is the earth rate vector in the desired initial orientation of the platform

and  $\underline{D}$  is the drift vector representing the drift of of each gyro.

From equation (2.6) the angular velocity of the stable member axes becomes

$$\underline{W}_{sm} = -\dot{A} \text{rot} \underline{W} + \gamma^{*-1} \text{mis} \underline{D} \quad (2.8)$$

Thus it can be seen that the only effect of the IRIG misalignments is to cross-couple the drifts between the axes; the effect of cross-coupling of earth rate by the misalignment of the gyros is canceled out by the stabilization loops.

Writing out equation (2.8) and neglecting the IRIG misalignments as insignificant

$$\begin{aligned} W_{xsm} &= -W_x + D_x - A_z W_y + A_y W_z \\ W_{ysm} &= -W_y + D_y - A_x W_z + A_z W_x \\ W_{zsm} &= -W_z + D_z - A_y W_x + A_x W_y \end{aligned} \quad (2.9)$$

Equation (2.9) is a set of coupled linear first order differential equations that can easily be solved by means of the Laplace transform. The general solution involves constants and sine and cosine functions of (earth rate) (t). The sine and cosine functions are expanded in power series and the  $t^2$  and higher terms are neglected to get the following set of equations:

~~CONFIDENTIAL~~

$$\begin{aligned}A_x(t) &= A_{x0} + (D_x - W_x - W_y A_{z0} + W_z A_{y0})t \\A_y(t) &= A_{y0} + (D_y - W_y - W_z A_{x0} + W_x A_{x0})t \\A_z(t) &= A_{z0} + (D_z - W_z - W_x A_{y0} + W_y A_{x0})t\end{aligned}\tag{2.10}$$

where  $A_{x0}$ ,  $A_{y0}$ , and  $A_{z0}$  are the initial errors in aligning the platform to the desired orientation.

The "standard model" that is examined in this thesis has the platform axes (x, y, z) initially oriented vertical, south and east.  $W_h$  and  $W_v$  will denote the horizontal and vertical components of earth rate at the latitude of the test site; hence,  $W_x = W_v$ ,  $W_y = -W_h$  and  $W_z = 0$ .  $g$  will denote local gravity.  $A_{x0}$  is the gyrocompassing error (with a maximum value of  $7 \times 10^{-3}$  rad);  $A_{y0}$  and  $A_{z0}$  are the vertical erection errors ( $4 \times 10^{-4}$  rad, maximum).

With this definition of the standard model, the platform rotation angles become

$$\begin{aligned}A_x(t) &= A_{x0} + (D_x - W_v + W_h A_{z0})t \\A_y(t) &= A_{y0} + (D_y + W_h + W_v A_{z0})t \\A_z(t) &= A_{z0} + (D_z - W_v A_{y0} - W_h A_{x0})t\end{aligned}\tag{2.11}$$

Now it remains to determine the relationship between PIPA output and gyro drift.

~~CONFIDENTIAL~~

## 2.2 PIPA Outputs

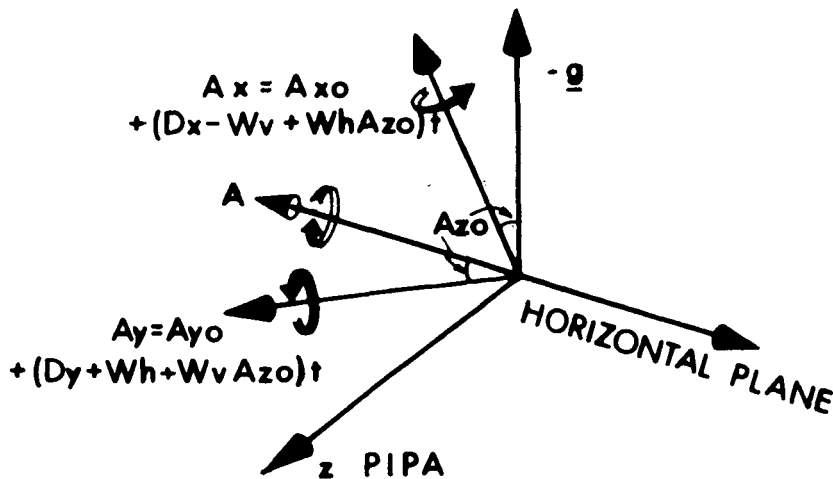
Now that the relationship between platform motion and IRIG drift is known, this motion must be measured if we are to determine the drift. The average PIPA pulse rate output is a function of the acceleration along its input axis. For the moment we shall neglect PIPA outputs due to launch vehicle sway.

First, it is obvious that the vertical (x) PIPA does not contain extractable information about the drift since any angular deviation of the PIPA from the vertical will always result in less of a pulse rate. The horizontal PIPAs may be of use. Consider an initial misalignment  $A_{zo}$  - what is the east PIPA output? For small angles

$$\frac{dN}{dt} = \frac{g}{H} A \quad (2.12)$$

where  $A$  is the angle that the PIPA makes with the horizontal plane.

From the following diagram we may determine  $A$





The angle A is given by the vector sum of the small angles Ax and Ay:

$$A(t) = A_{yo} + (Dy + Wh + WvAzo)t + (Axo + (Dx - Wv + WhAzo)t)Azo \quad (2.13)$$

Neglecting the insignificant terms in (2.13) we have

$$A(t) = A_{yo} + AxoAzo + (Dy + Wh)t \quad (2.14)$$

If we can determine the coefficient of the (t) term we have a measurement of the drift of the south gyro. What has helped us in the cancellation of the term WvAzo. No such cancellation will occur if a similar analysis is done on the south PIPA and that accelerometer's output is useless. The east PIPA output rate is

$$\frac{dN}{dt} = (A_{yo} + AxoAzo) \frac{g}{H} + B + (Dy + Wh) \frac{g}{H} t \quad (2.15)$$

where B is the uncompensated PIPA bias.

Integrating this equation will determine the PIPA pulse count as a function of time. Let N equal the pulse increment after the first pulse is measured and (t = 0) denote the time that the first pulse is measured after the platform goes inertial; then

$$N(t) = c \frac{g}{H} t + (Dy + Wh) \frac{gt^2}{(2H)} \quad (2.16)$$

is the equation that is to be solved for the drift of the south gyro. Clearly, the expression is parabolic and fitting a parabola to the pulse count at two times would determine the coefficient of the  $t^2$  term. A number of similar platform positions are required if we are to determine the drift coefficients of each gyro. The next section will introduce the error sources in any test configuration, then the following section will describe some simulated tests which proved that parabolic curve fitting is not an acceptable solution under conditions of base motion.

### 2.3 Error Sources

This section will consider all of the possible error sources in a drift coefficient test as was proposed in the previous section.

PIPA Quantization. The maximum velocity storage in each PIPA is the amount contained in one pulse. This quantization effect is due to the counting of a PIPA register at some time other than when the PIPA register actually changed. The resulting error can be eliminated by programming the AGC to store the actual time a register changed and its new reading. This is the only method of measurement considered in this thesis.

PIPA Scale Factor. The PIPA scale factor can have a maximum variation of 100 parts per million when an acceleration is being sensed. This error is due to variations in resistors, temperature, voltages, calibration error, and variation in torque pulse characteristics. The error will be assumed normally distributed about some bias point which is due to the temperature effect.

Timing Errors. Since there may be possible advantages in computer speed and storage if we do not require an extremely accurate reading of time, a maximum error of one millisecond in the measurement of time will be considered as the error in a reading.

PIPA Bias. All of the uncompensated accelerometer errors are combined into a maximum PIPA bias error of .2 cm/sec/sec. As was shown in the previous section, PIPA bias has a negligible effect on the test method.

~~CONFIDENTIAL~~

Mechanical Misalignment Errors. The gyro and accelerometer sensing axes are misaligned from an ideal orthogonal set because of errors in machining the platform faces, mounting errors, and errors in the inertial components themselves. Additional errors result from nonorthogonality of the gimbals and sensing resolver misalignments. These effects are negligible on the accuracy of the test procedure since they are of a bias nature.

Stabilization Loop Errors. The stabilization loop errors consist of steady state and dynamic errors in the stable platform orientation due to gimbal unbalances and stiction, amplifier nulls, and the stabilization amplifier bias. Even with these errors the loops can maintain the platform at the same inertial attitude within a five arc second tolerance. Since the loops are practically perfect, the assumption of a dynamically exact platform is a good one.

Nonlinear Terms. The assumption of a linearized model is good only for small initial misalignments of the platform and short test times. As an estimate only, we could expect the linearized analysis to be good (one meru accuracy in determining drift) for about ten minutes. This conclusion is based on an examination of the possible errors involved due to the simplification of the transformation matrix and the dropping of higher order terms in the linear model.

Wind Induced Missile Sway. The total PIPA pulse count at any instant of time is also dependent on the total velocity increment of the base during the period of the test.

$$N(t) = cgt/H + (Dy + Wh)gt^2/(2H) + v/H \quad (2.17)$$

~~CONFIDENTIAL~~

where  $v$  = the velocity increment in the direction of the east PIPA. If the effects of velocity are not included in equation (2.17) then an additional error is introduced. Since the missile remains on the launch pad, a reasonable first attempt at a solution of the problem is to consider the velocity effect to be a random measurement error; this will be considered in Section 2.4.

The maximum expected root mean squared displacement of the Apollo command module due to pad winds is about 10 cm. (ref. 4). This figure, of course, is based on a number of factors which are not yet well defined. In particular, the resonant frequency of the launch vehicle (Saturn 5) is estimated as .33 cycle/sec when fueled, .8 cycle/sec unfueled. If the dynamics of the missile are approximated by a second order system, a damping ratio of .1 in response to wind accelerations has been considered as typical. The characteristics of the wind are important too; the 10 cm. rms sway is for 95% probable winds at Cape Kennedy.

All of the preceding factors must be taken into consideration in determining a gyro drift test method. The next section will describe some experiments that were performed to see if we could neglect the velocity component along the east stable member axis.

#### 2.4 Least Squares Curve Fitting

$$N(t) = cgt/H + (Dy + Wh)gt^2/(2H) \quad (2.18)$$

From this equation it is possible to measure the drift deterministically. Consider the platform to go inertial at  $(t = 0)$  and the PIPA registers set equal to zero. At two later times  $(t_1, t_2)$  two pulse counts are recorded which is a sufficient condition to determine the drift. How would base motion affect the test?

The maximum pulse count due to a sinusoidal sway of amplitude 14 cm. is given by

$$\Delta N_{\max} = (14)(2\pi/3 H) \approx 5 \text{ pulses}$$

An error in  $N$  is related to an error in determining  $Dy$  as

$$\Delta N_{\max} = \Delta Dy t^2 g/(2H)$$

Assuming  $t = 360 \text{ sec}$ ,  $g = 980 \text{ cm/sec}^2$ ,  $H = 5.85 \text{ cm/sec/pulse}$ , we find that

$$\Delta Dy \approx 10 \text{ meru}$$

A deterministic drift test will not work under conditions of missile sway. This method is the only one that has been previously considered for use in the Apollo System. We should mention that the test is fairly effective in the laboratory.

The first attempt at finding an improved drift test method is to apply the method of least squares curve fitting to equation (2.18). The maximum likelihood estimate of the drift is the least squares estimate for the case of normally distributed errors with no previous information about the drift.

Let us rewrite equation (2.18) as

$$N = a_0 t + a_1 t^2 \quad (2.19)$$

where our particular problem is to find the "best" value of  $a_1$ . In particular, choose  $a_1$  so that

$$\sum_{j=1}^n (N_j - a_0 t_j - a_1 t_j^2)^2 \quad (2.20)$$

is least.

Differentiating partially with respect to  $a_0$  and  $a_1$  we obtain

$$\begin{aligned} \sum (N_j - a_0 t_j - a_1 t_j^2) t_j &= 0 \\ \sum (N_j - a_0 t_j - a_1 t_j^2) t_j^2 &= 0 \end{aligned} \quad (2.21)$$

The set of equations that is to be solved for  $a_1$  is

$$\begin{aligned} a_0 \sum t_j^2 + a_1 \sum t_j^3 &= \sum N_j t_j \\ a_0 \sum t_j^3 + a_1 \sum t_j^4 &= \sum N_j t_j^2 \end{aligned} \quad (2.22)$$

The two equations can be solved for a new  $a_1$  after each  $N_j$  is measured, or the data can be stored until the desired number of measurements has been made.

By means of the simulation programs described in Chapter 3, PIPA output data for the standard model was generated under laboratory and launch pad test conditions. The computer programs included the error sources described in the previous section. Under laboratory conditions, the test results for a least squares curve fit were excellent. PIPA output

~~CONFIDENTIAL~~

data was measured approximately every 20 seconds for a period of six minutes and processed at the end of that time to determine the drift. An accuracy of within one meru of the actual drift was realized during all normal operating conditions.

Under conditions of 10 cm. rms sway, however, the error in determining the drift averaged about 5 meru. The test time was varied up to 10 minutes, the PIPAs were read as fast as every .5 seconds; and still, no accurate determination of drift was made. The conclusion, then, is that the velocity of the missile must be taken into consideration. Now the problem is to estimate two constants and a variable at the time of every measurement.

A convenient method of formulating the solution to the problem is the so-called "Kalman Filter." In this technique, each PIPA measurement is processed as it is made to form a new estimate of the constant term, the drift, and three variables due to the motion of the missile. The procedure makes full use of the AGC's capabilities to act as the data processor for the test. The remainder of this chapter is devoted to the application of optimum filter theory to the measurement of gyro drift and the derivation of the proposed test method.

~~CONFIDENTIAL~~

## 2.5 Recursive Measurement Theory

The remainder of this chapter will derive the proposed drift coefficient test procedure. The theory of optimal statistical filtering (or recursive measurement theory) is given in references 1, 2, and 3 and will be discussed only to the extent necessary to understand the results.

When the launch vehicle is subjected to wind induced motion, the bending dynamics will be approximated by a second order system. The specific force on the vehicle due to the wind is assumed to be produced by a random (white noise) process passed through a first order shaping filter to generate an exponentially correlated specific force. The consequences of these assumptions are examined in Chapter 3.

The problem at hand is five dimensional and can be characterized by a five component state vector

$$\underline{x} = \begin{bmatrix} d \\ c \\ v \\ p \\ (aw) \end{bmatrix} \quad (2.23)$$

and

$d$  is the sum of the horizontal component of earth rate and the drift of the south gyro (the coefficient of the  $t^2$  term in the east PIPA output).

$c$  is the coefficient of the  $t$  term in the expression for PIPA output.

$v$  is the component of the velocity of the missile on the launch pad that is measured by the east PIPA.

$p$  is the easterly component of missile displacement from a vertical position.

$(aw)$  is the wind specific force (or that part of the vehicle acceleration due to the wind).



A second order system represents the missile bending dynamics

$$\dot{v} = -Wn^2 p - 2ZWn v + (aw) \quad (2.24)$$

where  $Wn$  is the resonant frequency of the launch vehicle in the first bending mode

$Z$  is the damping ratio of the second order system

Hence, the state vector consists of two constant components and three variables. The system model is completely specified by the state vector. At any instant of time, however, a deviation state vector exists because the system model is not identical to that of the actual system.

$\underline{\delta x}$  is the deviation vector or the difference between the system and the system model.<sup>1</sup>

$\hat{\underline{\delta x}}$  will denote an estimate of the deviation vector. Letters with  $\sim$  will denote measured quantities and no  $\wedge$  or  $\sim$  over the letter will indicate true values of the quantity.

As each PIPA measurement is taken, a new deviation vector exists and the system model is corrected to include the new piece of data. Let primed quantities indicate values extrapolated from the last measurement and unprimed quantities values after a measurement; then

$$\hat{\underline{x}} = \hat{\underline{x}}' + \hat{\underline{\delta x}} \quad (2.25)$$

The estimation error  $\underline{e}$  immediately after a measurement is

$$\underline{e} = \hat{\underline{x}} - \underline{x} \quad (2.26)$$

or

$$\underline{e} = -\underline{\delta x} \quad (2.27)$$

---

<sup>1</sup> The deviation is allowed to be large since we have a linear system.

Also, define  $\underline{e}'$  as the error existing before a measurement. Then the definition of the correlation matrices for both  $\underline{e}$  and  $\underline{e}'$  is

$$\underline{E}^* = \overline{\underline{e} \underline{e}^T} \quad (2.28)$$

$$\underline{E}'^* = \overline{\underline{e}' \underline{e}'^T} \quad (2.29)$$

If  $\hat{N}$  is the expected pulse count at some time and is based on the extrapolated value of the last state vector, then there will be a measured deviation in the pulse count

$$\delta \tilde{N} = N - \hat{N} + \alpha \quad (2.30)$$

where  $N$  is the actual value and  $\alpha$  is the error in measurement.

We define a measurement vector  $\underline{b}$  such that

$$\hat{N} = \underline{b} \cdot \underline{\hat{x}}' = \underline{b}^T \underline{\hat{x}}' \quad (2.31)$$

The components of  $\underline{b}$  are the partial derivatives  $\hat{N}(t)$  with respect to the components of the state vector at the instant of measurement.

Since the system model is corrected after each measurement, the predicted value of  $\delta N$  is zero just before a measurement

$$\delta \hat{N}' = 0 \quad (2.32)$$

It will be shown later that the optimum estimate of the deviation vector at the instant of measurement is given by

$$\delta \underline{\hat{x}} = \underline{w} \delta \tilde{N} \quad (2.33)$$

and the new estimate of the state vector is

$$\underline{\hat{x}} = \underline{\hat{x}}' + \delta \underline{\hat{x}} \quad (2.34)$$

and the new correlation matrix becomes

$$\underline{\hat{E}} = \underline{\hat{E}}' - (1/a) (\underline{\hat{E}}' \underline{b}) (\underline{\hat{E}}' \underline{b})^T \quad (2.35)$$

where

$$a = \underline{b}^T \underline{\hat{E}}' \underline{b} + \overline{\boldsymbol{\alpha}^2} \quad (2.36)$$

$$\underline{w} = (1/a) \underline{\hat{E}}' \underline{b} \text{ the weighting vector} \quad (2.37)$$

and  $\overline{\boldsymbol{\alpha}^2}$  = the mean squared measurement error.

These results are for uncorrelated measurement errors.

After incorporating the measurement into the estimation procedure, the system model is changed and the state vector and the correlation matrix are integrated to the next measurement time.

With this brief introduction to the recursive formulation of the problem, the details will be discussed in the ensuing sections.

Figure 2-1 serves to illustrate the recursive nature of the problem.

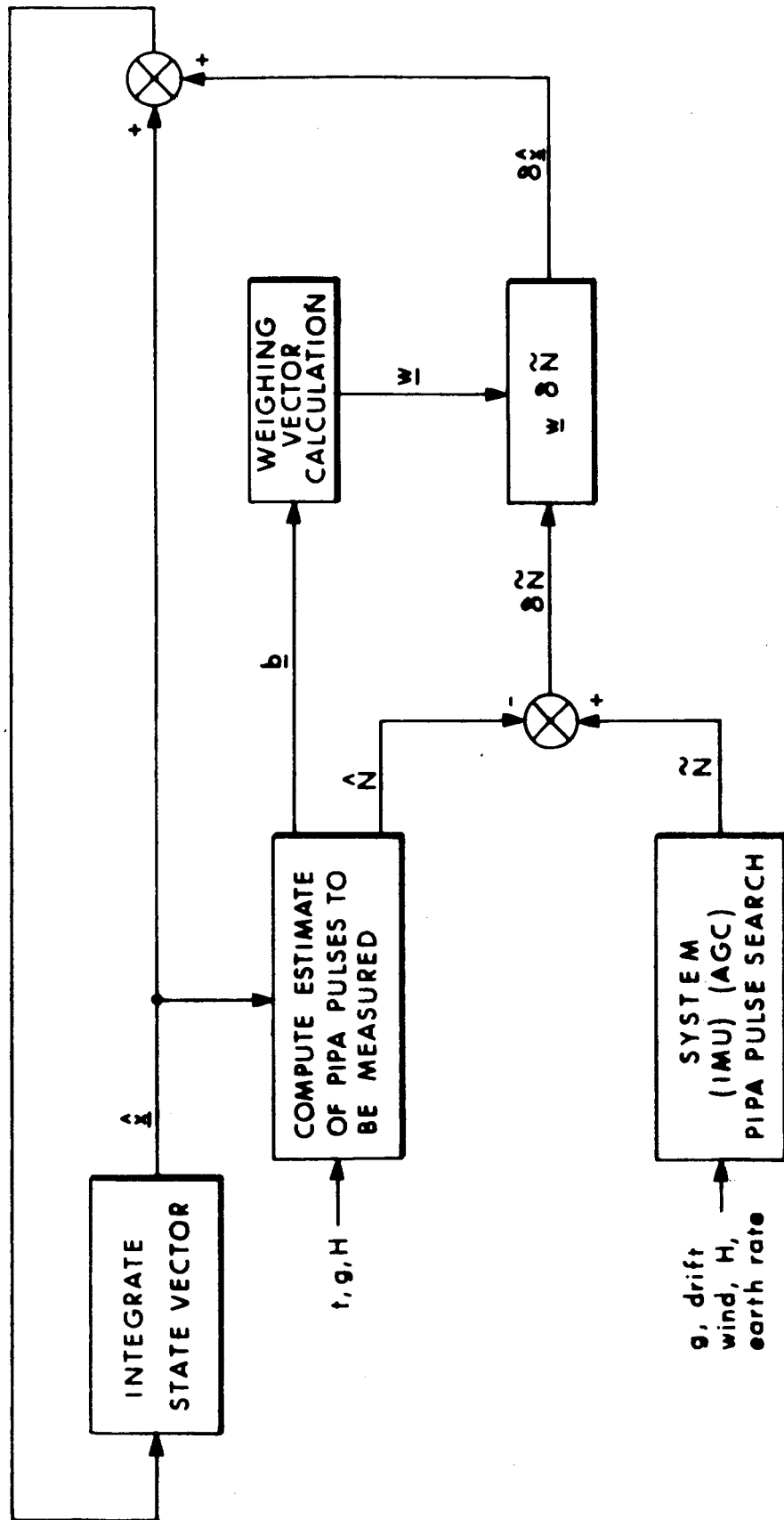


Figure 2-1 Recursive Operations

## 2.6 The Measurement Vector

The components of the measurement vector are the partial derivatives of  $\hat{N}(t)$  with respect to the components of the state vector.

Since

$$\hat{N}(t) = \hat{c} t g/H + .5 \hat{d} t^2 g/H + \hat{v}/H \quad (2.38)$$

then  $\underline{b}$  is defined as<sup>1</sup>

$$\underline{b} = \begin{bmatrix} .5t^2 g/H \\ t g/H \\ 1/H \\ 0 \\ 0 \end{bmatrix} \quad (2.39)$$

The components of  $\underline{b}$  are really sensitivity coefficients that relate how well a change in one of the state variables can be measured by the PIPA. Apparently, the measurement of gyro drift will be better for increasing test times. A six minute test has been chosen to satisfy this requirement and also to keep the assumption of linearized platform dynamics valid. Note that in general, a complete solution to the platform motion would have required coupling between the axes and the measurement vector would have been a measurement matrix since more than one PIPA would have been used. A complete solution of the linearized platform motion is not possible with the use of accelerometer information alone and this handicap will prevent us from measuring all of the drift coefficients individually. We will consider this problem later.

---

1 - In actual implementation the constant coefficients in  $\underline{b}$  would be incorporated into the state vector.

## 2.7 Measurement Error

The term  $c$  in the state vector represents the addition of another state variable to the state vector because the errors in PIPA output are indeed correlated with an infinite correlation time (PIPA bias, mis-alignments).<sup>1</sup> By defining  $c$  we estimate the correlated error as a state vector component and the remaining measurement errors are assumed random with zero mean.

We will have need of the following two equations

$$\overline{\alpha} = 0 \quad \text{PIPA pulses} \quad (2.40)$$

and

$$\overline{\alpha^2} = .25 \quad (\text{pulses})^2 \quad (2.41)$$

where the value for the mean squared measurement error  $\alpha^2$  has been experimentally determined as giving results that are consistent with the simulation studies.

Now that  $\underline{b}$  and  $\overline{\alpha^2}$  have been specified, the problem is to determine the weight that should be assigned to each measurement to update the estimate of the state vector and to find the errors in the estimate itself. It is implied and it will be shown that the optimal filter generates its own error analysis. The next section will derive the optimum weighing vector for any measurement and the resulting correlation matrix of estimation errors.

---

1 - A full discussion of the techniques for dealing with correlated measurement errors can be found in reference 1.

## 2.8 The Optimum Weighing Vector

We have previously stated the result that the optimum linear weighing vector takes on the form such that

$$\delta \hat{\underline{x}} = \underline{w} \delta \tilde{N} \quad (2.42)$$

$$\text{where } \underline{w} = (1/a) \underline{\hat{E}}' \underline{b} \quad (2.43)$$

and also the resulting correlation matrix is

$$\underline{\hat{E}}^* = \underline{\hat{E}}' - (1/a) (\underline{\hat{E}}' \underline{b}) (\underline{\hat{E}}' \underline{b})^T \quad (2.44)$$

$$\text{Define } \Delta \underline{\hat{E}}^* = (1/a) (\underline{\hat{E}}' \underline{b}) (\underline{\hat{E}}' \underline{b})^T \quad (2.45)$$

The mean squared error in the estimate of each state vector component is given by its respective term in the correlation matrix  $\underline{\hat{E}}^*$ .

We will first show that the vector  $\underline{w}$  has been chosen so that each component in the trace of the correlation matrix depends only on its corresponding term in  $\underline{w}$ . Since the trace represents the mean squared errors, then if  $\underline{w}$  is chosen to minimize the trace the mean squared error in each state vector component is minimized.

Use equations (2.26) and (2.34) to get

$$\underline{e} = \underline{\hat{x}}' + \delta \hat{\underline{x}} - \underline{x} \quad (2.46)$$

Then since

$$\delta \hat{\underline{x}} = \underline{w} \delta \tilde{N} \quad (2.47)$$

$$\delta \tilde{N} = N - \hat{N} + \alpha \quad (2.48)$$

$$\text{and } \hat{N} = \underline{b}^T \underline{\hat{x}}' \quad (2.49)$$

there follows by substitution in (2.46)

$$\underline{e} = \underline{e}' - \underline{w} \underline{b}^T \underline{e}' + \underline{w} \alpha \quad (2.50)$$

Assuming that  $\overline{e^{\prime}a}$  is zero and using the definition of the correlation matrices, it follows that

$$\underline{\dot{E}}^* = \underline{\dot{E}}^{\prime} - \underline{w} \underline{b}^T \underline{\dot{E}}^{\prime} - (\underline{w} \underline{b}^T \underline{\dot{E}}^{\prime})^T + a \underline{w} \underline{w}^T \quad (2.51)$$

Note that  $\underline{\dot{E}}^*$  and  $\underline{\dot{E}}^{\prime}$  are symmetric matrices and

$$a = \underline{b}^T \underline{\dot{E}}^{\prime} \underline{b} + \overline{a^2} \quad (2.52)$$

An inspection of the three right terms of equation (2.51) shows that the terms in the trace of  $\underline{\dot{E}}^*$  depend on only corresponding elements of  $\underline{w}$  and each term of the trace is then independent. Hence, if  $\underline{w}$  is chosen to minimize the trace of the correlation matrix, the mean squared error in each component of the state vector will be minimized.

From equation (2.51)

$$\text{trace}(\underline{\dot{E}}^*) = \text{trace}(\underline{\dot{E}}^{\prime} - 2 \underline{w} \underline{b}^T \underline{\dot{E}}^{\prime} + a \underline{w} \underline{w}^T) \quad (2.53)$$

To minimize equation (2.53), let the weighing vector  $\underline{w}$  have a variation  $\delta \underline{w}$ . Then, the variation in the trace of the correlation matrix  $\underline{\dot{E}}^*$  is given by

$$\delta \text{trace}(\underline{\dot{E}}^*) = 2 \text{trace}(\delta \underline{w} (a \underline{w}^T - \underline{b}^T \underline{\dot{E}}^{\prime})) \quad (2.54)$$

Setting equation (2.54) equal to zero, it follows that a stationary value for the trace is obtained if

$$\underline{w} = \frac{\underline{\dot{E}}^{\prime} \underline{b}}{a} \quad (2.55)$$

To show that equation (2.55) does yield a minimum, substitute for  $\underline{w}$  using the value we have just calculated plus  $\Delta \underline{w}$  and the trace will be found to increase for any  $\Delta \underline{w}$ .

The final results follow by substitution of equations (2.55) and (2.52) into equations (2.42) and (2.44)



$$\delta \underline{\hat{x}} = \underline{w} \delta \tilde{N} = \frac{\underline{\hat{E}}^* \underline{b} \delta \tilde{N}}{\alpha^2 + \underline{b}^T \underline{\hat{E}}^* \underline{b}} \quad (2.56)$$

$$\underline{\hat{E}}^* = \underline{\hat{E}}' - \frac{(\underline{\hat{E}}' \underline{b}) (\underline{\hat{E}}' \underline{b})^T}{\alpha^2 + \underline{b}^T \underline{\hat{E}}' \underline{b}} \quad (2.57)$$

where  $\underline{\hat{E}}^*$  is always less than  $\underline{\hat{E}}'$ ; hence a step decrease occurs in  $\underline{\hat{E}}'$  at every measurement.

and

$$\underline{\hat{x}} = \underline{\hat{x}}' + \delta \underline{\hat{x}} \quad (2.58)$$

We have now completely specified how a PIPA measurement is incorporated into the previous estimate of the state vector to form a new estimate. There remains the question of determining  $\underline{\hat{x}}'$  and  $\underline{\hat{E}}'$ ; the values of the estimated state vector and the correlation matrix that exist immediately before the measurement is made. The next section formulates these operations.

## 2.9 Extrapolation of $\hat{E}^*$ and $\hat{x}$

This section will derive the differential equations for the time variations of the estimated state vector and the correlation matrix. The AGC will be required to numerically integrate these equations between measurement times.

The following relationship is general

$$\dot{\underline{x}} = \underline{M}^* \underline{x}(t) + \underline{n}(t) \quad (2.59)$$

where  $\underline{n}(t)$  is a five-dimensional column vector that is a random (white) noise process such that

$$\overline{\underline{n}(t)} = 0 \quad (2.60)$$

Because we have assumed a perfectly instrumented platform and exact bending dynamics, the vector  $\underline{n}$  has zeros for its first four components. Then assume that

$$\frac{d(aw)}{dt} = \lambda (aw) + n(t) \quad (2.61)$$

i. e., the wind specific force is the result of a white noise process passed through a first order lag to generate an exponentially correlated specific force with correlation time of  $1/\lambda$  seconds.

Also,

$$\overline{\underline{n}(t) \underline{n}(\tau)^T} = \underline{N}^* \delta(t - \tau) \quad (2.62)$$

Since four components of  $\underline{n}$  are zero, the noise matrix  $\underline{N}^*$  has only one real term in it. In particular, denote this term by PD; it is equal to the white noise power density necessary to produce the desired root

mean square sway at the output of cascaded first and second order systems (the pseudo wind filter and the missile). Performing the necessary integrations, we find that

$$PD = \frac{4(\text{rms SWAY})^2 Z\lambda W_n^3 (W_n^2 + \lambda^2)^2 - (2Z\lambda W_n)^2}{(2ZW_n^3 + \lambda W_n^2 + \lambda^3 - 4Z^2 \lambda W_n^2)} \quad (2.63)$$

In particular, PD is a predetermined constant that is estimated from the conditions expected on the launch pad and is then stored in AGC memory.

To extrapolate the estimated state vector, the matrix  $\hat{M}^*$  is easily determined as

$$\hat{M}^* = \begin{bmatrix} 0 & 0 & 0 & 0 & 0 \\ 0 & 0 & 0 & 0 & 0 \\ 0 & 0 & -2ZW_n & -W_n^2 & 1 \\ 0 & 0 & 1 & 0 & 0 \\ 0 & 0 & 0 & 0 & -\lambda \end{bmatrix} \quad (2.64)$$

and clearly the extrapolation should be according to

$$\frac{d\hat{\underline{x}}}{dt} = \hat{M}^* \hat{\underline{x}}(t) \quad (2.65)$$

since the best estimate of  $\underline{n}(t)$  is zero. We should note that  $\hat{M}^*$  is a constant and also that only three of the components of  $\hat{\underline{x}}$  need be integrated.

The initial conditions on the integration are, of course, that

$$\hat{\underline{x}}(0) = \hat{\underline{x}}(t_j) \quad (2.66)$$

where  $\hat{\underline{x}}(t_j)$  refers to the last calculated value of  $\hat{\underline{x}}$ .

The extrapolation of the correlation matrix is a bit harder to derive. Write

$$\underline{\dot{E}}^* = \overline{\underline{e} \underline{e}^T}$$

and differentiate

$$\frac{d\underline{\dot{E}}^*}{dt} = \overline{\left(\frac{d}{dt} \underline{e}\right) \underline{e}^T} + \overline{\underline{e} \left(\frac{d}{dt} \underline{e}^T\right)} \quad (2.67)$$

Now

$$\begin{aligned} \frac{d}{dt} \underline{e} &= \underline{\dot{\hat{x}}} - \underline{\dot{x}} = \underline{\dot{M}} (\underline{\hat{x}} - \underline{x}) - \underline{\dot{n}} \\ &= \underline{\dot{M}} \underline{e}(t) - \underline{\dot{n}}(t) \end{aligned} \quad (2.68)$$

Hence

$$\begin{aligned} \underline{\dot{E}}^* &= \overline{(\underline{\dot{M}} \underline{e} - \underline{\dot{n}}) \underline{e}^T} + \overline{\underline{e} (\underline{e}^T \underline{\dot{M}}^T - \underline{\dot{n}}^T)} \\ &= \underline{\dot{M}} \underline{\dot{E}}^* + \underline{\dot{E}}^* \underline{\dot{M}}^T - \overline{\underline{n} \underline{e}^T} - \overline{\underline{e} \underline{n}^T} \end{aligned} \quad (2.69)$$

To evaluate  $\overline{\underline{e} \underline{n}(t)^T}$  write

$$\overline{\underline{e} \underline{n}(t)^T} = \overline{(\underline{\hat{x}} - \underline{x}) \underline{n}(t)^T} = \overline{\underline{\hat{x}}(t) \underline{n}(t)^T} - \overline{\underline{x}(t) \underline{n}(t)^T} \quad (2.70)$$

Clearly,  $\underline{\hat{x}}(t)$  and  $\underline{n}(t)$  are uncorrelated since  $\underline{\hat{x}}$  is extrapolated according to a noise-free model. Therefore,

$$\overline{\underline{e} \underline{n}(t)^T} = - \overline{\underline{x}(t) \underline{n}(t)^T} \quad (2.71)$$

Now

$$\underline{\dot{x}}(t) = \underline{\dot{M}} \underline{x} + \underline{\dot{n}}$$

so that

$$\underline{x}(t) = \int_{t_j}^t (\overset{*}{M} \underline{x}(\tau) + \underline{n}(\tau)) d\tau + \underline{x}(t_j) \quad (2.72)$$

Continuing

$$\begin{aligned} - \overline{\underline{x}(t) \underline{n}(t)^T} &= - \int_{t_j}^t \overline{(\overset{*}{M} \underline{x}(\tau) + \underline{n}(\tau) \underline{n}(t)^T)} d\tau - \overline{\underline{x}(t_j) \underline{n}(t)^T} \\ &= - \int_{t_j}^t \overline{(\overset{*}{M} \underline{x}(\tau) \underline{n}(t)^T)} d\tau - \int_{t_j}^t \overline{(\underline{n}(\tau) \underline{n}(t)^T)} d\tau - \overline{\underline{x}(t_j) \underline{n}(t)^T} \end{aligned} \quad (2.73)$$

But for  $\tau \leq t$  and  $t_j \leq t$  we have

$$\overline{\underline{x}(\tau) \underline{n}(t)^T} = 0 \quad \text{and} \quad \overline{\underline{x}(t_j) \underline{n}(t)^T} = 0$$

so that finally we obtain

$$\overline{\underline{e} \underline{n}(t)^T} = - \frac{1}{2} \overset{*}{N} \quad (2.74)$$

from the definition of the Dirac delta function ( $\delta$ ).

The end result is

$$\frac{d \overset{*}{E}}{dt} = \overset{*}{M} \overset{*}{E} + (\overset{*}{M} \overset{*}{E})^T + \overset{*}{N} \quad (2.75)$$

Where  $\overset{*}{N}$  has all zeros as elements except for the bottom right term which is PD. The initial condition on the integration is, of course, the value of the correlation matrix at the last measurement.

We need initial estimates of  $\underline{x}$  and  $\overset{*}{E}$  at the beginning of the test. They are as follows:

$$\hat{\underline{x}}(0) = \begin{bmatrix} (Wh + Dy) \\ 0 \\ 0 \\ 0 \\ 0 \end{bmatrix} \quad (2.76)$$

Where Dy is the estimate of the drift (if there was one) from previous tests and we have assumed no previous estimate of PIPA bias; also

$$\dot{\underline{E}}(0) = \begin{bmatrix} 10^{-12} & 0 & 0 & 0 & 0 \\ 0 & 2.5 \times 10^{-7} & 0 & 0 & 0 \\ 0 & 0 & (SWAY)^2 W_n^2 & 0 & 0 \\ 0 & 0 & 0 & (SWAY)^2 & 0 \\ 0 & 0 & 0 & 0 & (SWAY)^2 W_n^4 \end{bmatrix} \quad (2.77)$$

is a reasonable guess at maximum uncertainties in drift ( $\approx 14$  meru), misalignment, and the sway variables.<sup>1</sup>

We have now completely specified the data handling.

$$\left. \begin{aligned} \dot{\underline{x}} &= \underline{M} \underline{x} \\ \dot{\underline{E}} &= \underline{M} \underline{E} + (\underline{M} \underline{E})^T + \underline{N} \end{aligned} \right\} \begin{array}{l} \text{no} \\ \text{measurement} \end{array}$$

and

$$\left. \begin{aligned} \underline{x} &= \underline{x}' + \frac{\underline{E}' \underline{b} (\delta \tilde{N})}{\alpha^2 + \underline{b}^T \underline{E}' \underline{b}} \\ \underline{E} &= \underline{E}' - \frac{(\underline{E}' \underline{b}) (\underline{E}' \underline{b})^T}{\alpha^2 + \underline{b}^T \underline{E}' \underline{b}} \end{aligned} \right\} \begin{array}{l} \text{measurement} \end{array} \quad (2.78)$$

1 - If desired, the three terms due to vehicle motion in the initial correlation matrix can be set equal to zero for laboratory testing. The results, of course, will be the same.

In Chapter 3 the integration of  $\hat{\underline{x}}$  and  $\hat{\underline{E}}^*$  was carried out as follows: search for a PIPA pulse<sup>1</sup> if a pulse does occur, integrate  $\hat{\underline{x}}$  and  $\hat{\underline{E}}^*$  to the time of the pulse and proceed to form a new estimate of  $\underline{x}$ ; if no pulse occurs during a .1 second interval, integrate  $\hat{\underline{x}}$  and  $\hat{\underline{E}}^*$  over that .1 second time step. This method is summarized in Figure 2-2. The particular choice of a maximum time step such as .1 second between updates depends on the numerical accuracy desired. Also, in this scheme of pulse searching we are sure of detecting the natural frequency of the launch vehicle which is required if we are to estimate (filter) the variables due to the motion.

The figures following Figure 2-2 summarize the analytical results of Chapter 2.

---

1 - By pulse search we mean that the computer is triggered into computation when a PIPA pulse is recorded.

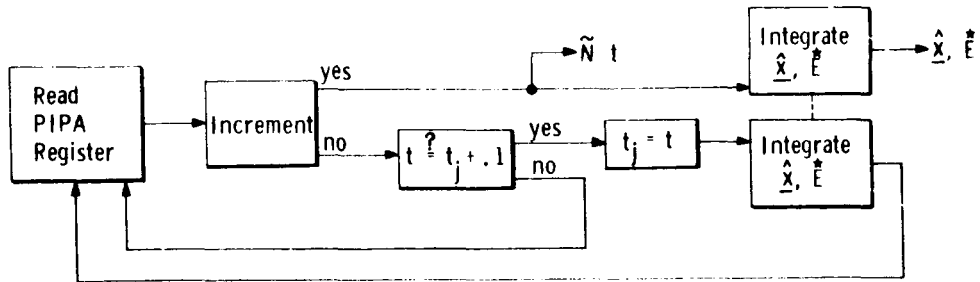


Figure 2-2 Pulse Search and Update

$$\hat{\mathbf{E}}(0) = \begin{bmatrix} 10^{-12} & 0 & 0 & 0 & 0 \\ 0 & 2.5 \times 10^{-7} & 0 & 0 & 0 \\ 0 & 0 & (\text{sway})^2 Wn^2 & 0 & 0 \\ 0 & 0 & 0 & (\text{sway})^2 & 0 \\ 0 & 0 & 0 & 0 & (\text{sway})^2 Wn^4 \end{bmatrix}; \quad \hat{\mathbf{x}}(0) = \begin{bmatrix} Wh + Dy \\ 0 \\ 0 \\ 0 \\ 0 \end{bmatrix};$$

$$\hat{\mathbf{M}} = \begin{bmatrix} 0 & 0 & 0 & 0 & 0 \\ 0 & 0 & 0 & 0 & 0 \\ 0 & 0 & -2ZWn & -Wn^2 & 1 \\ 0 & 0 & 1 & 0 & 0 \\ 0 & 0 & 0 & 0 & -\lambda \end{bmatrix}; \quad \hat{\mathbf{N}} = \begin{bmatrix} 0 & 0 & 0 & 0 & 0 \\ 0 & 0 & 0 & 0 & 0 \\ 0 & 0 & 0 & 0 & 0 \\ 0 & 0 & 0 & 0 & 0 \\ 0 & 0 & 0 & 0 & PD \end{bmatrix}$$

Initialization Constants:  $g, Wh, Dy, H, PD, \alpha, \hat{\mathbf{E}}(0), \hat{\mathbf{x}}(0), \hat{\mathbf{M}}, PD, \text{sway}(\text{rms}), \lambda, Z, Wn$

Figure 2-3 Initial Conditions



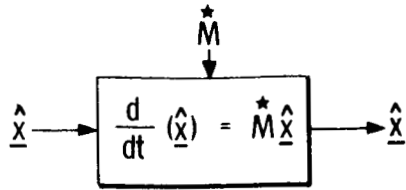


Figure 2-4 Integrate  $\hat{x}$

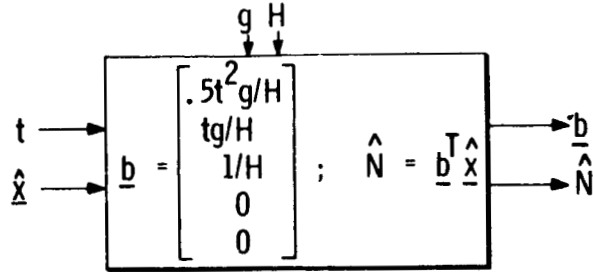


Figure 2-5 Compute  $\hat{N}$  and  $\underline{b}$

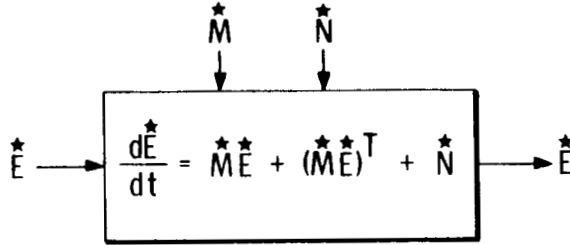


Figure 2-6 Integrate  $\hat{E}$

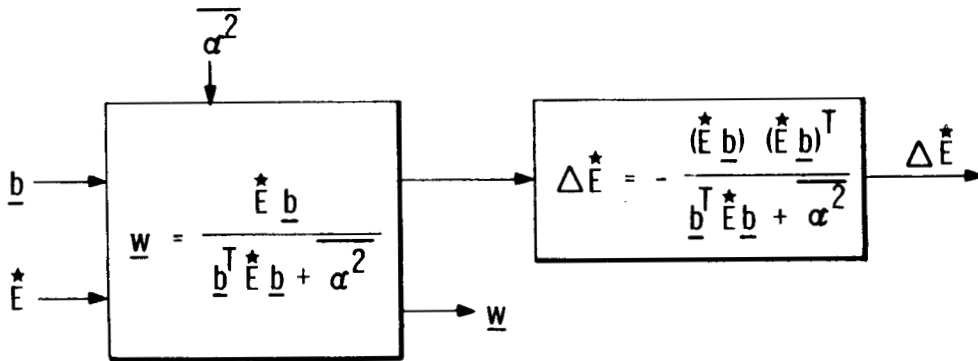


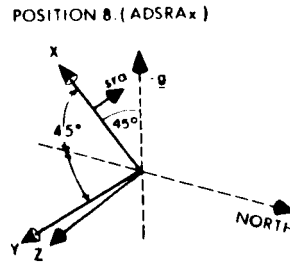
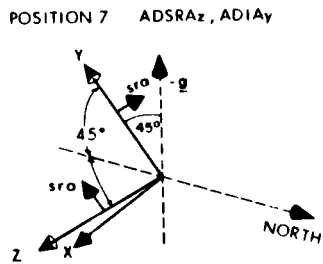
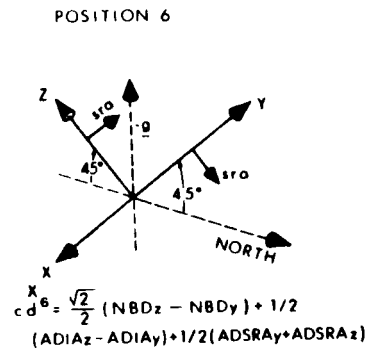
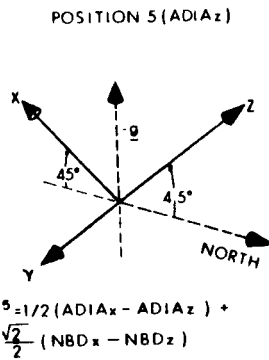
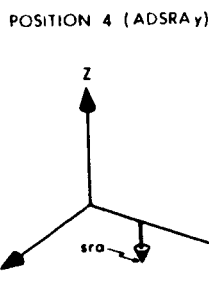
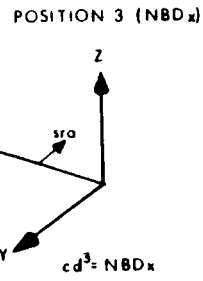
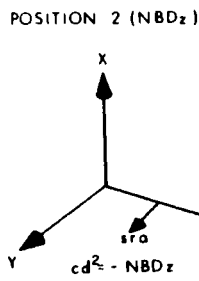
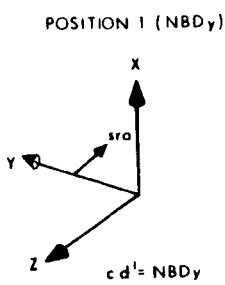
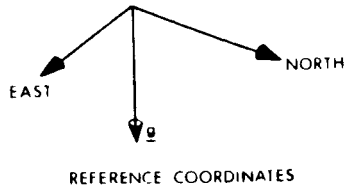
Figure 2-7 Compute Weighing Vector and Step Change in Correlation Matrix

## 2.10 Platform Positions

In this section we will present the eight initial platform positions required to determine the drift coefficients. The next section will review the estimation procedure and the necessary implementation.

The result of the recursive measurement scheme is an estimate of the sum of horizontal earth rate and drift of the south gyro. Therefore, the final step in the data processing is the subtraction of horizontal earth rate from (d) at the end of six minutes. The estimate of the drift is clearly unbiased.

Eight initial platform orientations are given in the following figure.  $(cd^i)$  will indicate the calculated drift from the measurement scheme  $(cd^i = \hat{d} - Wh)$  applied in each orientation. The y stable member cannot be positioned near the vertical because of the gimbal lock constraint.



$$cd^7 = \frac{\sqrt{2}}{2} (NBD_y + NBD_z) + 1/2 (ADIA_y - ADIA_z) + 1/2 (ADSRA_y + ADSRA_z)$$

$$cd^8 = 1/2 ADSRA_x + \frac{\sqrt{2}}{2} (NBD_y + NBD_z) + 1/2 (ADIA_x - ADIA_y)$$

$$cd^6 \cdot cd^7 = (ADSRA_z + ADSRA_y) + \sqrt{2} NBD_z$$

$$cd^7 - cd^6 = ADIA_y - ADIA_z + \sqrt{2} NBD_y$$

Figure 2-8 Test Positions

From these platform positions the drift coefficients can be calculated as is shown. Note that an apriori knowledge of ADIAx is required. The linear analysis does not permit an explicit calculation of the ADIA drift coefficients (in essence, rotations about the vertical). The general result of the thesis is, therefore, somewhat limited; however, the actual implementation of it is not expected to require much more computer programming than existing test methods.

Two possible methods are available if it is desired to measure the vertical gyro drift on the launch pad, however both require considerable implementation. The first is to attempt the complete nonlinear solution to the equations of motion for an untorqued platform; this is felt unrealistic. The second is to torque the platform and determine the drift as part of a platform alignment program; this procedure has been used in reference 5 with success. The author proposes that the test method developed here be used in conjunction with one platform position in which the referenced alignment program is used. Reference 5 is also an application of optimum statistical filtering.

In the eight position test we have proposed, the drift coefficients are calculated from the results of drift measurements in several platform positions as shown in Figure 2-7. Propagation of errors is then important. If we denote the rms error in  $(cd^i)$  by  $\sigma$  and assume  $\sigma$  is approximately the same for each position, then the

following equations may be derived for the rms uncertainty in any drift coefficient.

$$\begin{aligned}
 \sigma (\text{NBDy}) &= \sigma \\
 \sigma (\text{NBDx}) &= \sigma \\
 \sigma (\text{NBDz}) &= \sigma \\
 \sigma (\text{ADSRAy}) &= \sqrt{2} \sigma \\
 \sigma (\text{ADIAz}) &= \sqrt{8} \sqrt{\sigma^2 + \sigma^2 (\text{ADIAx})/8} \\
 \sigma (\text{ADSRAz}) &= \sqrt{6} \sigma \\
 \sigma (\text{ADIAy}) &= \sqrt{12} \sqrt{\sigma^2 + \sigma^2 (\text{ADIAx})/12} \\
 \sigma (\text{ADSRAx}) &= \sqrt{20} \sqrt{\sigma^2 + \sigma^2 (\text{ADIAx})/10}
 \end{aligned} \tag{2.79}$$

where  $\sigma^2 (\text{ADIAx}) =$  estimated mean squared error in determining ADIAx.

In the next chapter it is shown that  $\sigma \approx .3$  meru for any test. Assuming that  $\sigma (\text{ADIAx}) = .3$  meru, equation (2.79) may be evaluated as

$$\begin{aligned}
 \sigma (\text{NBDy}) &= .3 \text{ meru} \\
 \sigma (\text{NBDx}) &= .3 \text{ meru} \\
 \sigma (\text{NBDz}) &= .3 \text{ meru} \\
 \sigma (\text{ADSRAy}) &= .42 \text{ meru} \\
 \sigma (\text{ADIAz}) &= .85 \text{ meru} \\
 \sigma (\text{ADSRAz}) &= .74 \text{ meru} \\
 \sigma (\text{ADIAy}) &= 1.04 \text{ meru} \\
 \sigma (\text{ADSRAx}) &= 1.34 \text{ meru}
 \end{aligned} \tag{2.80}$$

Equation (2.80) is essentially the main result of the thesis. The rms uncertainty is seen to vary from .3 meru for the bias drifts

to 1.34 meru for the ADSRAX term. This is a considerable improvement over the estimated accuracy ( $\pm 50$  meru) of the existing test method.

## 2.11 Implementation

The two main concerns in determining the necessary implementation for application of the test procedure to the Apollo G&N System are required speed of data processing and computer storage that is needed.

The following table shows the computer time (in milliseconds) for arithmetic operations using the double precision interpreter.

Table 2-1 AGC (Block II) Arithmetic Operations (Ref. 8)

<u>Operation</u>	<u>Time</u>	<u>Operation</u>	<u>Time</u>	<u>Operation</u>	<u>Time</u>
Add	.66	Subtract	.66	Multiply	1.13
Divide	2.48	Sign Test	.70	Vector Add	.92
Vector Subtract	.92	Dot Product	3.08	Scaler x Vector	3.27
Vector/Scaler	5.39	Cross Product	4.98	Vector x Matrix	8.98
Matrix x Vector	8.98	(vectors and matrices 3 dimensional)			

In determining the time required for calculations by the computer we should remember that the correlation matrix is symmetric and only fifteen of its twenty-five elements need be integrated; that the state vector has only three components that must be integrated; that  $\underline{b}$  has only three real components; and  $\overset{*}{N}$  has only one non-zero element. These facts will be of help in the actual programming.

The author estimates that the processing of a measurement and the two integrations will require about .2 second each to complete.

A scheme that updates the state vector and correlation matrix only every .5 second is demonstrated as follows:

<u>Operation</u>	<u>Time</u>	<u>Time Running</u>
Pulse Found	0	0
Update (to 0)	.2	.2
Process Pulse	.2	.4
Pulse Search	.1	.5
Update (to .7)	.2	.7
Pulse Search	.3	1.0
Update (to 1.2)	.2	1.2
Pulse Search	.3	1.5
Update (to 1.7)	.2	1.7
Pulse Search	.3	2.0
Update (to 2.2)	.2	2.2

The computer will search for a pulse approximately 40% of the time (the computer is inactive until a pulse triggers it to start the update process). In applying the test procedure to systems with a computer that is not as sophisticated as the AGC there may be some question as to whether the data can be processed on board.

The presently programmed gyro drift test requires approximately 800 words of AGC memory. The author estimates a 20% increase in computer memory required for the gyro drift test if the proposed test procedure is implemented. The end result is a considerable increase in test accuracy.

The total test time for an eight position test including one alignment test from reference five (40 minutes) is about 82 minutes.



Added to this are the times required to align the platform to seven of the positions; the total test time is estimated as 2 hours maximum to determine all of the drift coefficients.

It is interesting to note that all three major functions of the AGC (platform alignment, component performance determination, and astronomical navigation) are now shown to have essentially the same statistical formulation.

## 2.12 Chapter Summary

In Chapter 2 we have motivated the development of a recursive measurement technique for determination of gyro drift. As each PIPA pulse count is registered, the estimates of the state vector and the correlation matrix undergo step changes. Between measurements the estimates are integrated according to our estimate of vehicle dynamics. A total of six minutes of data processing in each of seven test positions and one alignment test (40 minutes) will allow us to determine all of the IRIG drift coefficients. It has been estimated that this test procedure will require a 20% increase in existing computer storage and the total test time will be about two hours.

## CHAPTER 3

### COMPUTER SIMULATIONS

In this chapter the simulation studies that were carried out in the Computation Center of the Instrumentation Laboratory are described. The effects of different error sources on the drift test are studied and found to be minor. The test procedure measures the drift of the south gyro in the standard platform orientation with a rms uncertainty of three tenths of a meru under launch pad environments.

### 3.1 Computer Program Description

Revisions were made to existing Apollo G&N System simulations in order to accommodate the test procedure. In these programs the system variables were completely updated every tenth of a second and extrapolated between updates to second order accuracy. The author's desire was to duplicate as closely as possible actual data and data rates that would be available from the system under a variety of environments. The capability to study the effects of different error sources was included. These programs are on file in the computation center.<sup>1</sup> The wind specific force was generated by a random binary process passed through a digitally simulated shaping filter. The total PIPA pulse count due to the horizontal accelerations, earth rate and gyro drift, is thought to be an extremely accurate representation of what could be expected from the actual system.

The recursive measurement procedure was included in these programs as a subroutine and the output of any particular run could be either data, graphs, or punched cards. The graphs that are presented were all done by the computer with the author superimposing a number of runs in order to make parametric studies.

Appendix "A" serves to demonstrate in one program the computation routines that are needed if we are given PIPA pulse count as a function of time. The next section will present the simulation results.

---

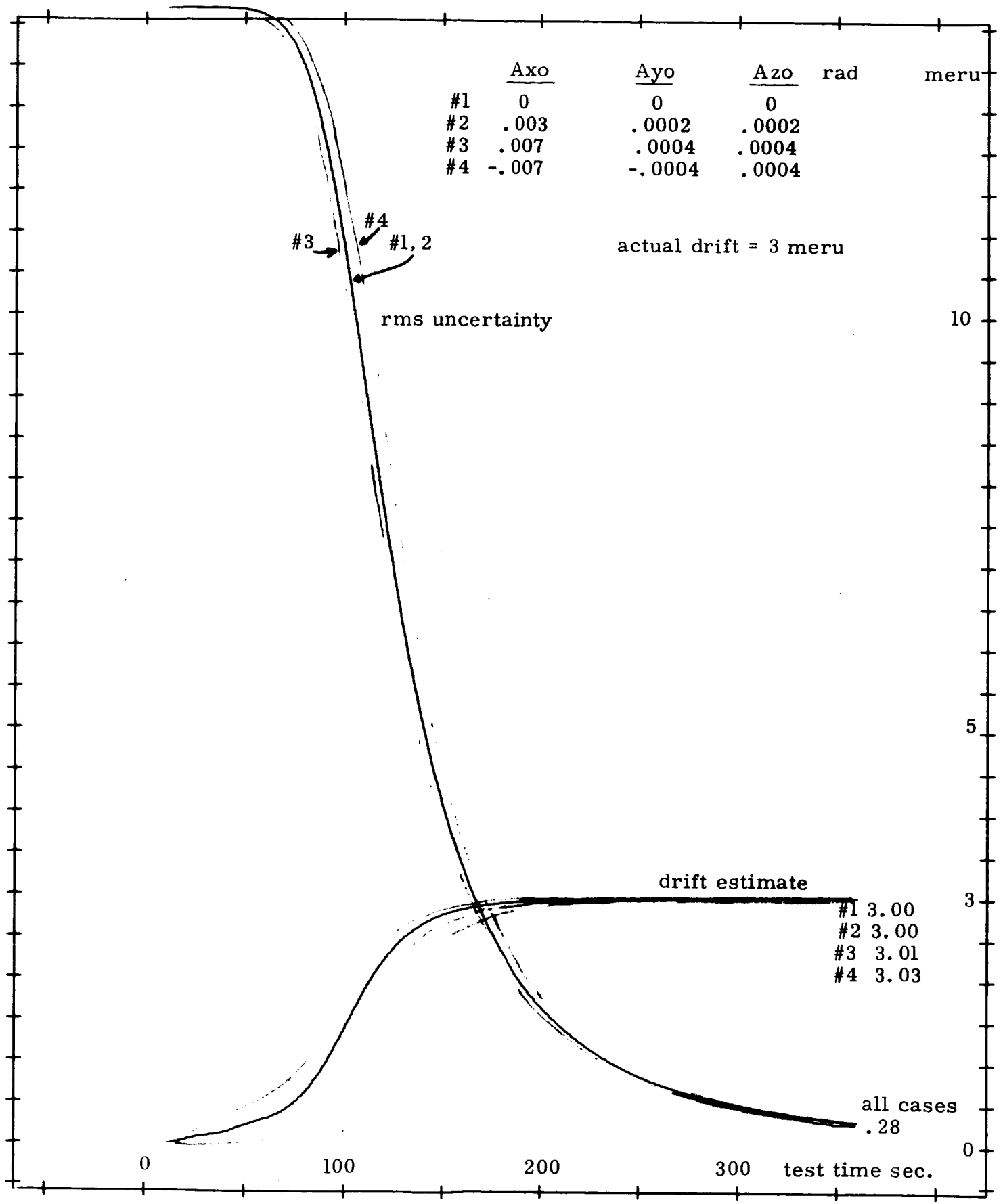
<sup>1</sup> ENVCIPISEARCH, IMUCDUPISEARCH, PRELAUNCH on file in IL-7.

### 3.2 Simulation Results

This section will present the results of the computer simulations. Arbitrary values of drift were assigned to the x, y, and z gyros - 10, 3, and 10 meru, respectively. The results of this section will show that an extremely effective test has been developed for the determination of the y gyro drift under both laboratory and launch pad conditions.

Platform Initial Misalignments (Graph #1). The estimate of the y gyro drift can be seen to be excellent and varying only slightly as a function of initial misalignments. The different initial estimation rates are due to the change in the term (c) caused by the different misalignments; the final error in the estimation is a function of the non-linear terms which begin to appear as time increases. The time varying nature of the statistical estimation technique decreases the effects of misalignments because the gains in the filter decrease with time while the non-linear terms are increasing with time. The shifting of the rms uncertainty curves reflect the changes in the bias term caused by the different values of Ayo.

~~CONFIDENTIAL~~



Graph #1 Effects of Misalignments

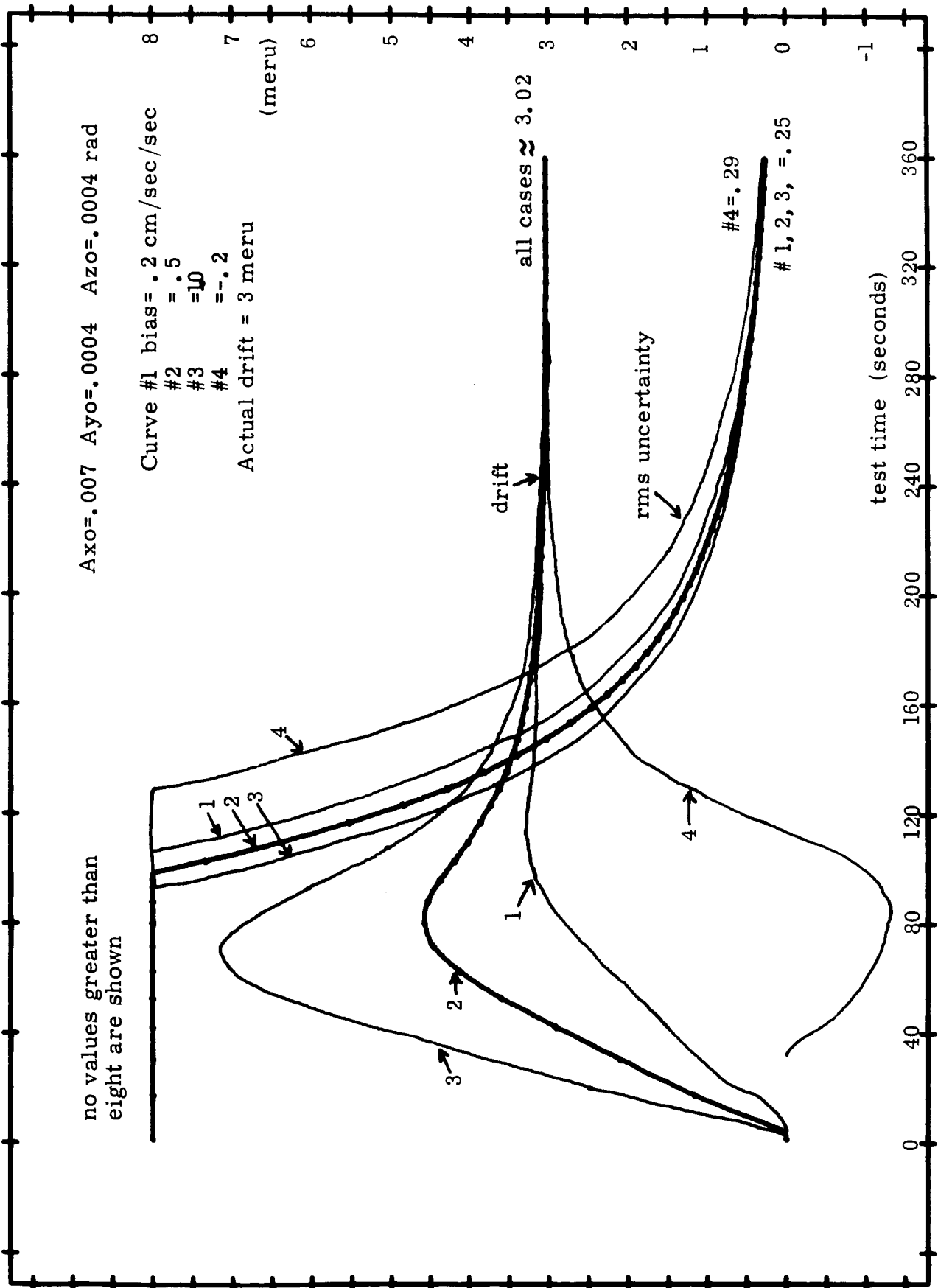
~~CONFIDENTIAL~~

PIPA Bias (Graph #2). The effects of PIPA bias are to introduce different initial estimation rates and corresponding rates of decrease of the rms uncertainty curves. As we would expect, a positive increase in bias will increase the initial estimation rate and increase the rate at which the rms uncertainty decreases since more pulses are processed. The transient peaks reflect the dynamics of the estimation procedure.

PIPA Scale Factor and Timing Errors. Both of these effects have been found to contribute a negligible error to the drift estimation. This conclusion is based on a number of computer runs using all expected scale factor errors and a timing uncertainty ( $3\sigma$ ) of 1 millisecond.

Effect of Incorrect  $\overline{\alpha^2}$  (Graph #3). Since scale factor errors and timing errors have a negligible effect on the results, we can expect the correct value of  $\overline{\alpha^2}$  to be close to zero. This graph shows that the final estimation of drift is essentially independent of our choice of  $\overline{\alpha^2}$ . The rms uncertainty, of course, will depend directly on  $\overline{\alpha^2}$ . From this graph and a number of similar computer runs, a choice of a much smaller measurement variance is justified for laboratory testing. However, the author has chosen the larger value of .25 pulse<sup>2</sup> so that the resultant dispersion of results for launch pad testing will agree with the rms uncertainty predicted from the measurement scheme. This will be discussed shortly.

~~CONFIDENTIAL~~

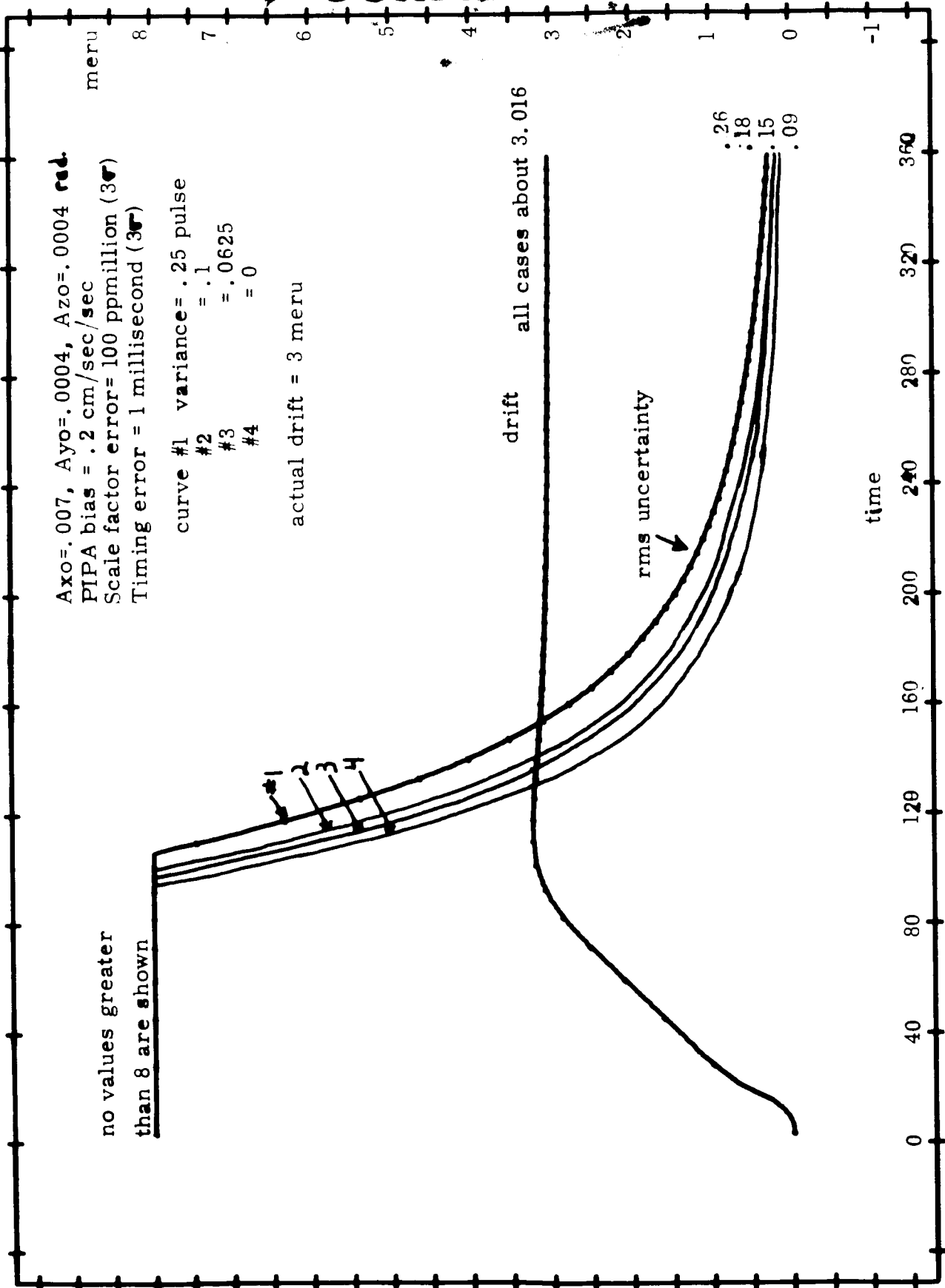


~~CONFIDENTIAL~~

Graph #2 Effects of PIPA Bias



~~CONFIDENTIAL~~



Graph #3 Incorrect Measurement Variance

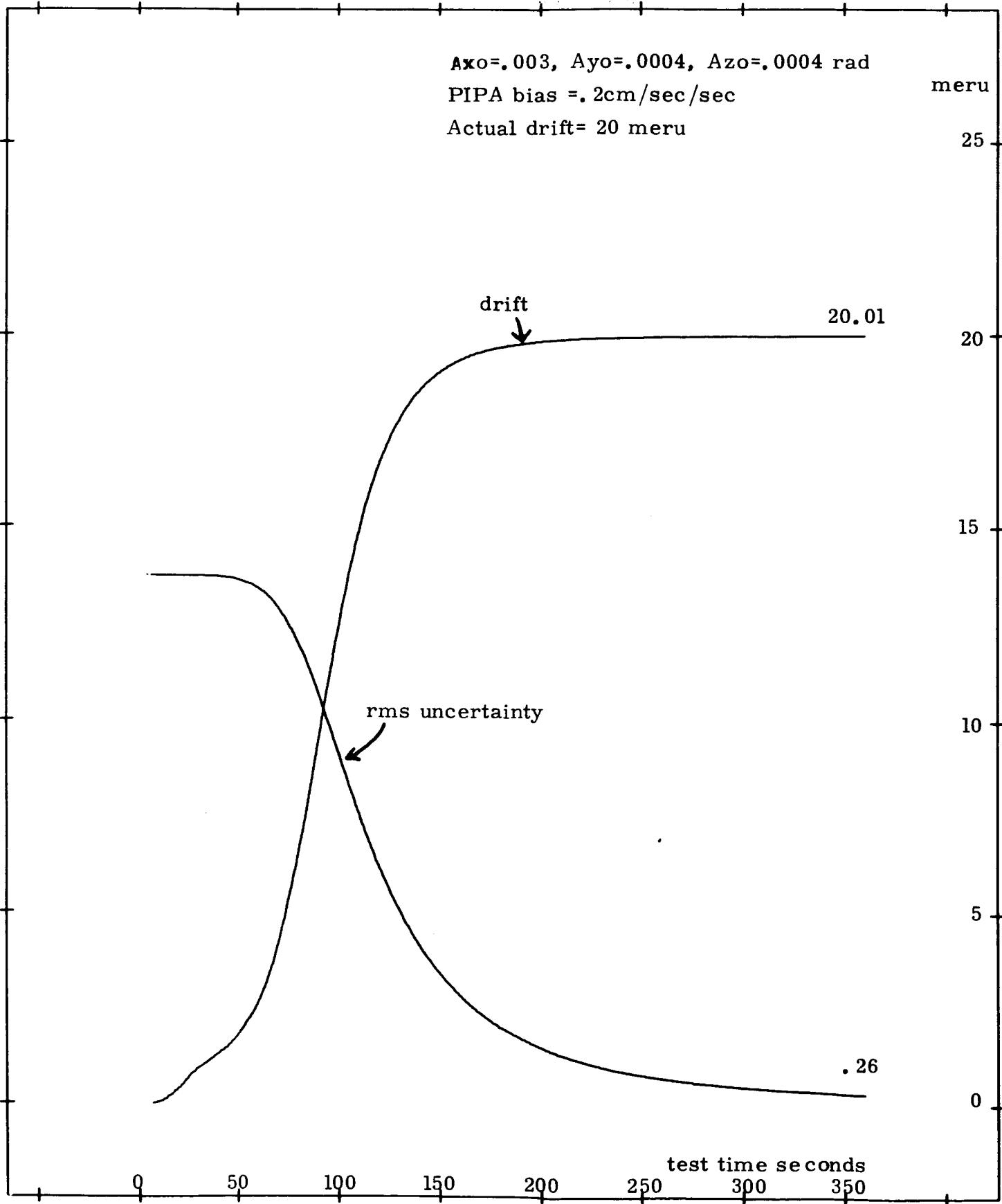
~~CONFIDENTIAL~~

Incorrect Initial Correlation Matrix (Graph #4). Using a value of 14 meru for the rms uncertainty in the initial estimate of zero drift, a computer run was made with an actual drift of 20 meru. As we can see, the value of the initial correlation matrix does not affect the final estimated value of drift.

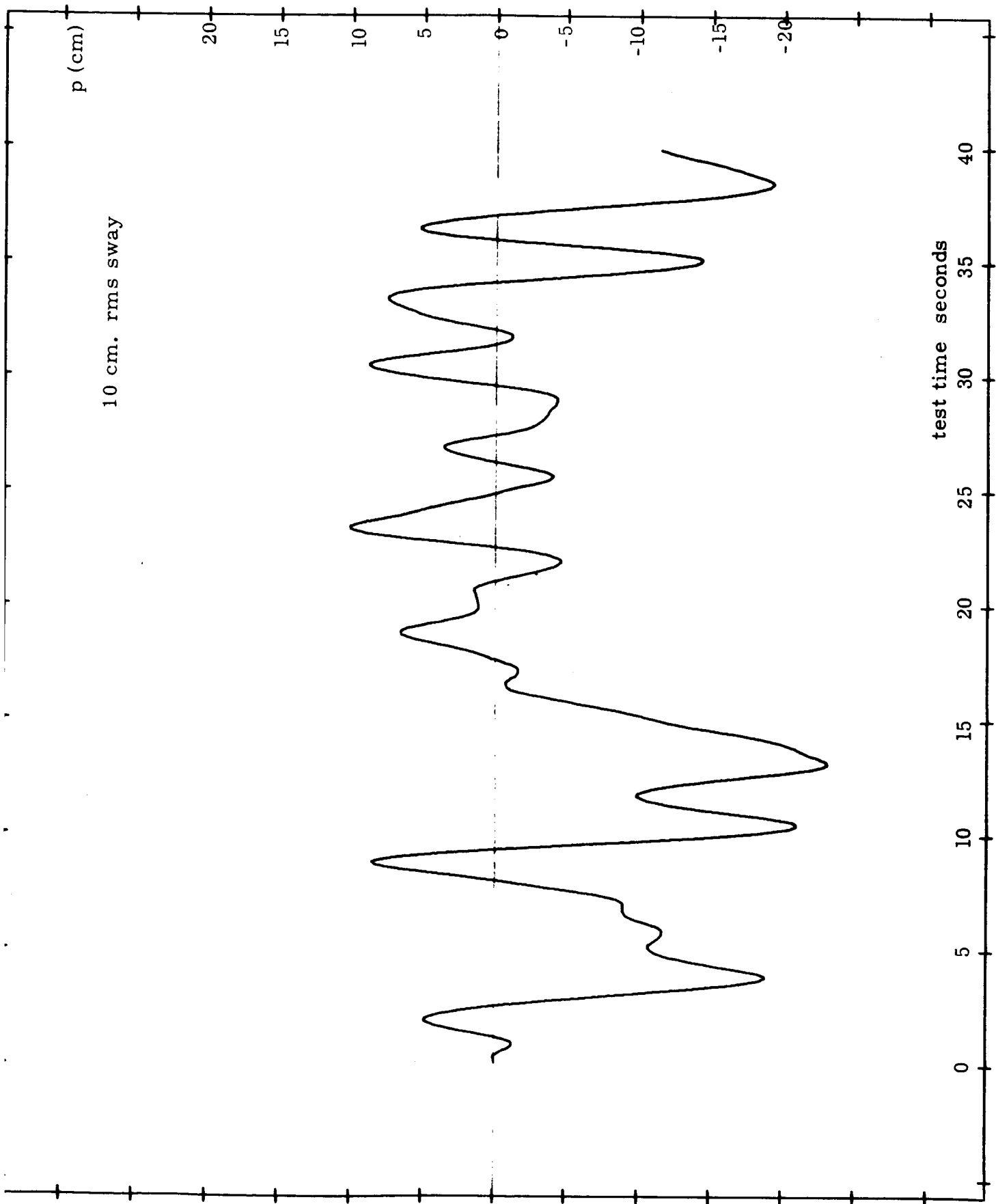
Missile Motion (Graph #5). A typical time history of the easterly displacement of the launch vehicle for 40 seconds of a six minute test in which the rms displacement is 10 cm. is given in this graph.

Velocity Estimation (Graph #6). This graph shows the actual velocity, the extrapolated velocity, and the estimated velocity at selected intervals during a launch pad test. This graph really serves to show the amplitude of the interfering velocity.

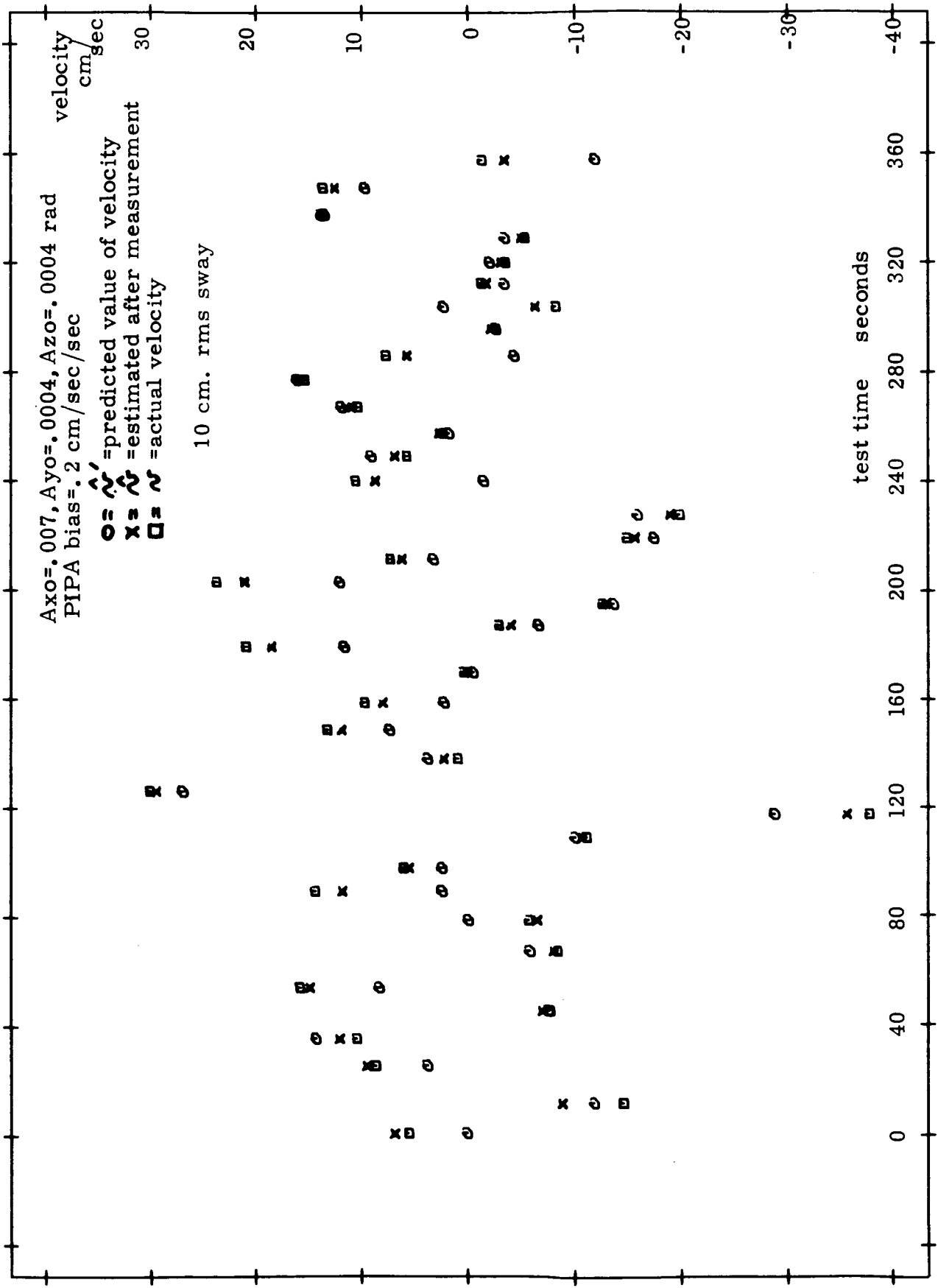
Launch Pad Estimation (Graph #7). This graph shows the typical transients experienced in the drift estimation for a launch pad test with the 10 cm. rms motion. After about four minutes of filtering most of the transients have disappeared and the estimated value settles out. The graph demonstrates the time varying nature of the filter. The following list of drift estimates and rms uncertainties is the result of a number of computer runs with different random processes used to generate the 10 cm. rms sway.



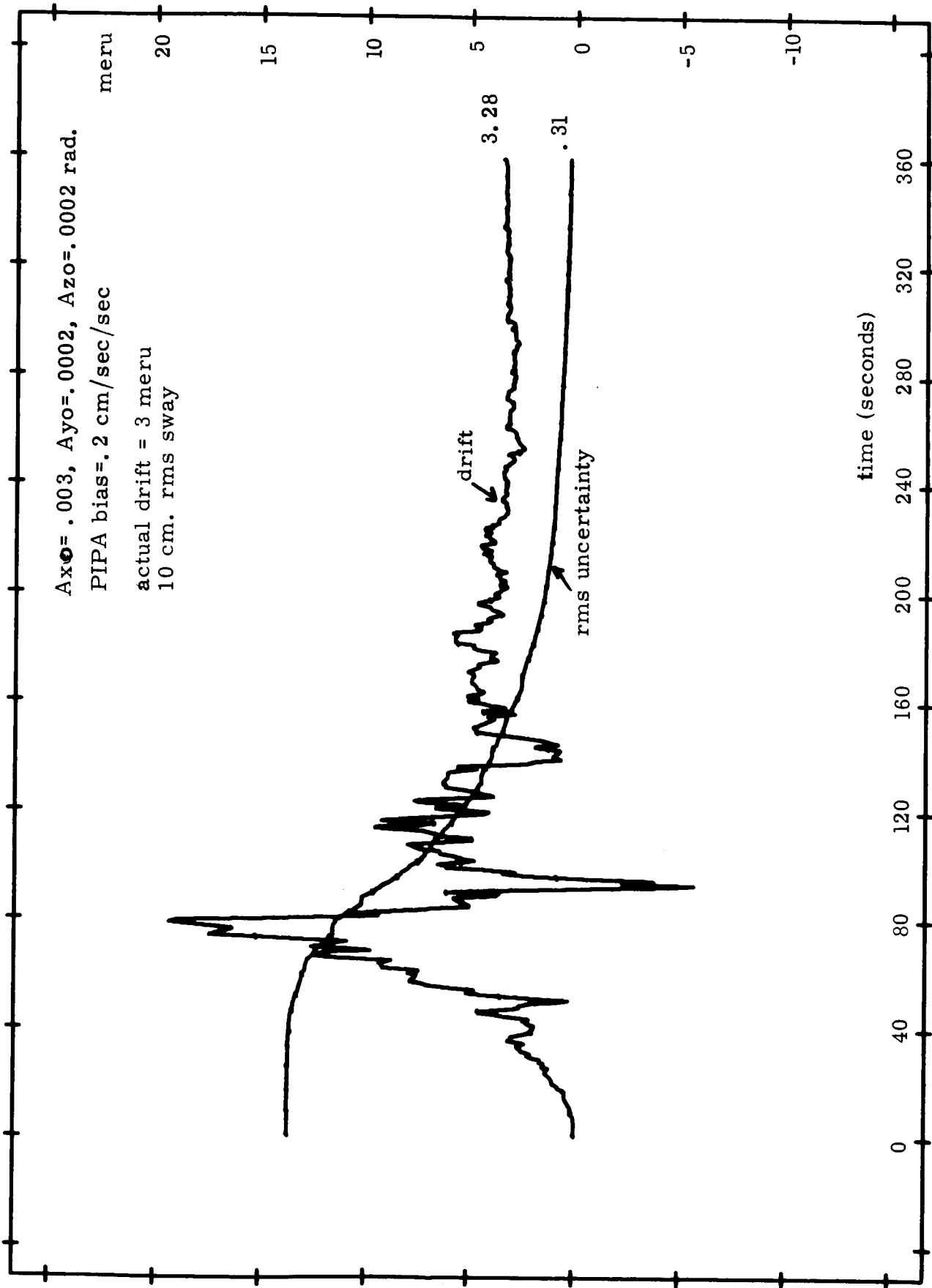
Graph #4 Incorrect Initial Correlation Matrix



Graph #5 Missile Motion



Graph #6 Velocity Estimation



$Ax = .003$ ,  $Ayo = .0002$ ,  $Azo = .0002$  rad.  
PIPA bias = .2 cm/sec/sec  
actual drift = 3 meru  
10 cm. rms sway

time (seconds)

Graph #7 Launch Pad Estimation

~~CONFIDENTIAL~~

<u>Estimated Drift (meru)</u>	<u>Uncertainty - rms</u>
3.28	.31
2.96	.31
2.74	.33
2.93	.32
3.16	.30
3.48	.31
3.08	.29

This short list is used to justify the choice of  $\alpha^2$  as .25 pulse<sup>2</sup> so that the actual launch pad results will show a dispersion which is more in accord with the estimated uncertainties.<sup>1</sup>

Incorrect Wind Correlation Time. The following list shows that the effect of variations in actual wind correlation time do not cause very much error in the drift estimation. This is a hoped-for result since the characteristics of the launch pad winds are not well defined.

<u>Wind Correlation Time (sec)</u>		<u>Estimated</u>	<u>Uncertainty</u>
<u>Model</u>	<u>Actual</u>	<u>Drift</u>	<u>rms</u>
10	5	3.29	.26
10	10	3.28	.31
10	20	3.51	.34
10	100	3.09	.40

Variations in Wn. A greater dependence of the results on the actual value of launch vehicle resonant frequency can be seen in the following list. Launch pad sway-vibration measurements will be needed to firm up our estimate of Wn for the system model.

<sup>1</sup> The mean value of drift for the seven runs is 3.09 meru; the standard deviation is .23 meru.

~~CONFIDENTIAL~~

<u>Resonant Frequency (rad/sec)</u>	<u>Estimated</u>	<u>Uncertainty</u>	
<u>Model</u>	<u>Actual</u>	<u>Drift</u>	<u>rms</u>
2.07	1.02	2.42	.38
2.07	2.07	3.28	.31
2.07	5	3.27	.24
2.07	6.28	2.76	.23
2.07	9.42	4.82	.23

Variations in Damping Ratio. The quality of drift estimation shows less of a dependence on damping ratio than on  $W_n$ . However, a good estimate of  $Z$  from vibration tests can be made and it will be to our advantage to use the best information available.

<u>Damping Ratio</u>	<u>Estimated</u>	<u>Uncertainty</u>	
<u>Model</u>	<u>Actual</u>	<u>Drift</u>	<u>rms</u>
.1	.05	3.06	.27
.1	.1	3.28	.31
.1	.2	3.39	.34
.1	.3	3.29	.35
.1	.4	3.35	.35
.1	.5	2.96	.36
.1	.6	2.54	.36

rms Sway Greater than 10 cm. Two runs with a 15 cm. rms sway were made. The model was not corrected and the results show that no major problem can be expected from greater than normal sway amplitudes.

<u>Estimated Drift</u>	<u>rms Uncertainty</u>
3.34	.28
2.99	.28



### 3.3 Conclusions from the Simulation Studies

In the previous section the results of a number of computer simulations have been presented which indicate that the test procedure will be an extremely accurate one under all specified environments and error sources. The rms uncertainty in any test will be about .3 meru for the determination of the south gyro drift. The only further information needed is a better knowledge of the launch vehicle dynamics. This type of information is easily gathered by sway and vibration measurements once the launch vehicle is in place (ref. 7). In conclusion, the use of computer simulations has played an important part in determining the effectiveness of the proposed gyro drift coefficient test. The results have shown an extremely effective test under many different operating conditions.

~~CONFIDENTIAL~~

## CHAPTER 4

### CONCLUSION AND SUMMARY

A linearized model of an inertial platform has been developed in order to relate accelerometer outputs to gyroscope drift. After eliminating deterministic and curve fitting drift tests, an optimum statistical filter is proposed for use during a launch pad system test to determine the IRIG drift coefficients. By means of computer simulations the effectiveness of the test procedure was examined and found to be a significant improvement over existing test procedures. The increase in computer storage is estimated at 20% and the total test time is about 2 hours to determine all of the IRIGs' drift coefficients. In order that the test be as effective as is intended, additional studies are recommended in order to define the launch vehicle sway characteristics.

The drift of the south gyro in the standard platform orientation can be determined with a root mean square uncertainty of three tenths of a meru. The coefficients of all the gyros may be determined by a series of eight platform positions; one position is an alignment test position. The resultant uncertainties may vary up to 1.34 meru; these errors are due to the propagation of calculation errors since the drift coefficients are calculated from a number of previous measurements of the south gyro drift.

~~CONFIDENTIAL~~

With this thesis and reference 5, the complete problem of drift measurements, when the system is on the launch pad, has been discussed using optimum filtering. The author considers the problem well solved and the next step is the actual application of these techniques of the Apollo System.

## APPENDIX A

### DEMONSTRATION PROGRAM USING THE MAC LANGUAGE

The following two pages demonstrate the typical calculations that must be made to determine the drift of the south gyro. The program is written in the MAC computer programming language. Data cards punched with the time of the measured PIPA pulse count and the pulse count are needed as inputs to the program. This program is similar to that used in the simulation studies.

```

*      USERFILE=DISCFILE
*      MAC#  GTS
M      DIMENSION 5
E      * *      -
M      RESERVE M,NOISE,0

R      INITIALIZATION SECTION

M      BEGIN  READ G,H,L,DY,PRBIS
R      GRAVITY,SCALE FACTOR,LATITUDE,PREVIOUS ESTIMATES OF DRIFT AND BIAS
M      READ W ,Z,LAMBD,SWAY
S      N
R      NATURAL FREQ.,DAMPING RATIO,INVERSE WIND CORR. TIME,EXPECTED RMS SWAY
M      VAR=.25,TLAST=0
E      L=DEGTORAD(L)
S      -5
E      W =7.292115(10-5),W =W COS(L),MRU=.001W
S      E      H      E      E
E      -
S      X=((W +DY MRU),(PRBIS H/G),0,0,0)
S      H
E      *      -12 -      -7 -      2      2 -      2 -      4      2
M      E=(10-12,0,2.5(10-7),0,(W SWAY2),0,SWAY2,0,(W SWAY2))
S      N      N
E      PD=4 SWAY2 Z LAMBD W3 ((W +LAMBD)2 - (2 Z LAMBD W)2)
S      N      N      N
E      PD=PD/( 2 Z W +LAMBD W3 +LAMBD2 -4 Z LAMBD W )
M      N      N      N
R      NOISE POWER DENSITY REQUIRED TO PRODUCE THE SWAY
M      NOISE =PD
S      24
E      2
M      M12 =-2ZW ,M13 =W ,M14 =1,M17 =1,M24 =-LAMBD
R      CONSTANT MATRIX IN THE DIFF.EQN. FOR THE STATE VECTOR

R      INPUT DATA CARDS ARE TIME THEN PULSE COUNT
M      LOOP  READ TNEW,N
M      IF TNEW ZERO,EXIT
M      T=TLAST,DT=.1
E      IF (TNEW-TLAST-.1)NEG,DT=(TNEW-TLAST)
S      * * *
M      UPDATE ME=M E
R      EXTRAPOLATE THE CORR. MATRIX AND STATE VECTOR TO THE TIME OF MEAS.
E      * * * *
M      DE/DT=ME+TRANSPOSE( ME)+NOISE
S      - * -
E      DX/DT=MX
M      * -
M      DIFEQ T,DT,DE/DT,DX/DT
M      IF DQPHASE NZ,GO TO UPDATE
M      IF T=TNEW,GO TO IML
M      IF (TNEW-T-.1)POS,DT=.1,GO TO UPDATE
M      IF(TNEW-T-.1)NEG,DT=TNEW-T,GO TO UPDATE

```

R  
E  
M  
E  
M  
E  
R  
E  
M  
E  
R  
E  
M  
E  
R  
M  
S  
M  
R  
M  
M  
M  
\*  
\*  
\*

CALCULATION SECTION

```

-
IML      B=(.5TTG/H,TG/H,1/H,0,0)
THE MEASUREMENT VECTOR
- * -
      INVRA=B.(EB)+VAR
- * -
      WEIGH=(1/INVRA)EB
THE WEIGHING VECTOR
- -
      NESTM=B.X
ESTIMATED PULSE COUNT
- -
      DELST=WEIGH(N-NESTM)
- - -
      X=X+DELST
NEW STATE VECTOR
- * -
      C=EB
* *      --
      E=E-(1/INVRA)CC
NEW CORRELATION MATRIX
      DRIFT=(X -W )/MRU,RMSUN=SQRT(E )/MRU
              0 H              0
      PRINT DRIFT,RMSUN,T
DRIFT    RMS UNCERTAINTY    TIME
      TLAST=T
      GO TO LOOP
      START AT BEGIN

RUN
DATA CARDS
ENDJOB

```

## REFERENCES

1. Battin, R. H., Astronautical Guidance, McGraw-Hill Book Company, Inc., New York, N. Y., 1964.
2. Levine, Gerald, Application of Midcourse Guidance Technique to Orbit Determination, MIT Instrumentation Laboratory Report E-1261, December, 1962.
3. Kalman, R. E. and Bucy, R. S., "New Results in Linear Filtering and Prediction Theory," *Journal of Basic Engineering*, March, 1961.
4. MIT/IL Report E-1061, AGANI, November, 1962(Confidential).
5. Brock, L. D., Application of Statistical Estimation to Navigation Systems, Ph.D. Thesis, MIT Department of Aeronautics and Astronautics, June, 1965 (to be published as T-414 by MIT/IL).
6. Farmer, R., "Apollo Fine Align Mode Specification," ACSpark Plug Memo XDE 34-S-6, February, 1964 (Confidential).
7. Barrieau, R. A., "Sway Measurements of Gemini Spacecraft," MIT/IL Apollo System Test Group Memo #298, December, 1964.
8. Muntz, C. A., Users Guide to the Block II AGC/LGC Interpreter, MIT Instrumentation Laboratory Report R-489, April, 1965.
9. Laats, A., "Gyro Coefficient Measurement," MIT/IL Apollo System Test Group Memo #354, February, 1965.